Hydrological Processes

WILEY

RESEARCH ARTICLE OPEN ACCESS

Tracing Flow Pathways of Nutrients in Dairy Farms—An End Member Mixing Analysis Approach

Jonah Lee Bas[1] | Andrew W. Western[2] | Perran Cook[3] | Ziming He[2] | Wei Wen Wong[3] | Robert Sargent[1] | Anna Lintern[1]

[1]Department of Civil and Environmental Engineering, Monash University, Clayton, Victoria, Australia | [2]Department of Infrastructure Engineering, The University of Melbourne, Parkville, Victoria, Australia | [3]Water Studies, School of Chemistry, Monash University, Clayton, Victoria, Australia

Correspondence: Jonah Lee Bas (jonah.bas@monash.edu)

Received: 20 February 2026 | **Revised:** 2 June 2026 | **Accepted:** 5 June 2026

Keywords: eco detection ion-Q+ | end member mixing analysis | first flush | flood irrigation | hydrologic connectivity | nutrient export | surface runoff

ABSTRACT

Understanding dominant transport pathways of nutrients is crucial for designing and implementing effective mitigation strategies to reduce downstream water quality impacts. This study applied a novel high frequency nutrient and major ion analyser and end member mixing analysis (EMMA) using conservative tracers to identify dominant flow pathways and their influence on nitrogen and phosphorus transport from two dairy farms in the Macalister Irrigation District, Victoria, Australia. Analyses show that farm drain water at both farms was consistently a mixture of event water (rainwater and irrigation water) and soil water, which represent surface runoff and shallow subsurface soil flow, respectively, with limited contribution from groundwater. The dominance of end members varied between farms and events and was controlled by surface roughness, microtopography, and antecedent soil moisture. Nutrient-to-chloride ratios revealed that nitrate and phosphate have a pronounced "first flush" behaviour during events when surface runoff is dominant, indicating rapid mobilization of nutrients from manure. In contrast, events when shallow subsurface soil flow was dominant are associated with low nutrient export. These results showed the role of surface runoff in driving nutrient export from low-relief dairy farms and highlight the importance of irrigation management, surface roughness preservation, and reuse systems for reducing nutrient losses from flood-irrigated dairy regions.

1 | Introduction

The transport of nutrients from heavily irrigated dairy farming regions poses a critical threat to the environment, as excess nutrients from these regions contribute to the degradation of water quality of downstream water bodies and groundwater resources (Carpenter et al. 1998; Hoekstra et al. 2020; McDowell et al. 2023; Oenema and Oenema 2021). These regions are considered critical sources of nitrogen (N) and phosphorus (P) due to the large quantities of cattle excreta in paddocks and laneways, as well as the concentration of these nutrients in confined areas such as dairy sheds and effluent ponds (Aarons et al. 2023; Chalar et al. 2017; Galloway et al. 2018). When high nutrient loads reach surface water bodies, it can lead to eutrophication, harmful algal blooms, hypoxia, and loss in biodiversity (Dai et al. 2023; Smith et al. 1999), while groundwater contamination can lead to risks in drinking water quality and human health (Adimalla et al. 2019; Xiao et al. 2021).

Understanding the transport of nutrients from agricultural landscapes requires identifying transport via several flow pathways such as surface runoff, subsurface flow, and groundwater flow (Darracq et al. 2008; Destouni et al. 2010; Edith Allaire et al. 2011; Hofmeister et al. 2022; Liu et al. 2020). These pathways differ in transport timescales and connectivity, influencing the timing and magnitude of nutrient export (Lindgren et al. 2007; McGrath et al. 2009; Peterson et al. 2011). Understanding which nutrient transport pathways are dominant is therefore crucial for designing and implementing effective mitigation strategies such as vegetation buffers, improved irrigation practices, or nutrient application timing.

Several catchment-scale studies have attempted to disentangle flow pathways of nutrients using various methodologies such as hysteresis analysis of concentration-discharge (C-Q) relationships, hydrograph separation, statistical methods, and physically-based models (Adams et al. 2020; Ford et al. 2019; Hofmeister et al. 2022; Mackie et al. 2021; Porter et al. 2022; van der Salm et al. 2012; van Meter and Basu 2017; Wan et al. 2023; Wild-Allen and Andrewartha 2016; Williams et al. 2018; Wu et al. 2017). While these approaches were able to disentangle nutrient flow pathways, they also suffer from certain limitations. For instance, hysteresis analysis cannot quantify contributions of distinct water sources and long-term statistical methods require extensive meteorological, hydrological, and nutrient datasets. Hydrograph separation techniques that used older mixing analysis methods were unable to determine conservative tracers and the number of end members.

A promising alternative that may overcome these limitations is the combined use of end member mixing analysis (EMMA) by Christophersen and Hooper (1992) and diagnostic tools of mixing models by Hooper (2003) and Liu, Bales, et al. (2008). This method can identify multiple water sources that drain into an outlet and quantify the relative contributions of these sources using conservative environmental tracers such as chloride, sodium, or potassium. In fact, several studies have utilised mixing approaches (including EMMA) to disentangle nutrient transport processes across diverse landscapes from tile drained agricultural catchments to forested headwater catchments (e.g., Bernal et al. 2006; Bujak-Ozga et al. 2025; Hofmeister et al. 2022; McHale et al. 2002; Mulholland and Hill 1997; Nazari et al. 2021; Van Gaelen et al. 2014; van Verseveld et al. 2008).

In intensively managed, heavily irrigated dairy farms, the presence of irrigation infrastructure, fertilizer and effluent application, as well as high stocking rates can create complex water and nutrient interactions. Examining this complexity during rainfall and irrigation events is the main focus of this paper. This study aims (1) to identify the dominant flow pathways that contribute to farm drain discharge during rainfall and irrigation events using end member mixing analysis and (2) to investigate how these flow pathways influence nutrient transport during such events. By identifying flow contributions and linking them with nutrient transport under various flow conditions, this study can provide insights into when and how nutrients are mobilized and exported from fields, which in turn will help enable targeted management strategies in similar dairy-dominant landscapes.

2 | Materials and Methods

2.1 | Study Area

The study was conducted on two dairy farms within the Macalister Irrigation District (MID) in Gippsland, Victoria. The MID is located in the flat region of the Lake Wellington Catchment with an elevation ranging between 30 and 50 masl. The mean annual precipitation in the MID averages from 600 to 650 mm surrounding the upstream Lake Glenmaggie gauge but reduces to 400–600 mm in the lower plains around the Thomson-Macalister basins. The mean annual temperature ranges from 18°C to 24°C. Maximum temperatures typically occur in the summer months (December–February) with very minimal rainfall, during which farming operations are supplemented by irrigation water fed by Lake Glenmaggie in the north and the Thomson and Macalister Rivers, as well as on-farm reuse systems. The primary land use at the MID is dairy (~90%) with small portions of non-dairy livestock enterprises, cropping, and horticulture (West Gippsland Catchment Management Authority 2018).

Two dairy farms—Dairy Farm 1 (DF1) and Dairy Farm 2 (DF2)—were selected for this study. Their approximate locations with respect to the MID are shown in Figure 1a. The outlet points at both of these sites are located on farm drains. Based on the Australian Soil Classification scheme, both farms are underlain with Dermosols (Suborder AA) and Sodosols (Suborder AB).

The monitoring site at DF1 receives drainage from a total area of 19.3 ha encompassing 20 paddocks with areas ranging from 1 to 2 ha each. The property had a milking herd of approximately 250 cows in 2024 but it has been as high as 320 cows in previous years and the total property area is 73 ha. An area of around 2 ha is grazed per day on predominantly white clover (*Trifolium repens*) and perennial ryegrass (*Lolium perenne*) pastures. Several types of irrigation are used on the farm, such as flood irrigation, fixed sprinklers, and bike shift sprinklers. However, flood irrigation is used exclusively on the paddocks that drain to the monitoring site. Effluent is also applied on selected paddocks, but not to those within the study catchment.

The monitoring site at DF2 has a drainage area of 14.4 ha with 8 paddocks measuring approximately 2.4 ha each. The property has a milking herd of approximately 500 cows and has a total property area of 120 ha. Similar to DF1, flood irrigation is used exclusively on the paddocks that drain to the monitoring site at DF2 and are predominantly perennial ryegrass (*L. perenne*) and white clover (*T. repens*) pastures. Both DF1 and DF2 apply urea-based fertilizers at a rate of approximately 60–90 kg/ha/yr. as N.

2.2 | Data Collation

2.2.1 | Tracer Concentrations of Potential End Members

Four potential end members—rainwater, irrigation water, soil water, and groundwater—were identified to contribute water at the outlet points at DF1 and DF2. These end members were identified based on prior knowledge and field observations at the study sites. Rainwater and irrigation water were collected during sampling campaigns between 2021 and 2022. Soil water was extracted using a soil water suction sampler with a depth of 0.3 m below the soil surface. Groundwater samples were collected from bores and wells (with average depths to water table from 1 to 5 m) throughout the Macalister Irrigation District in close proximity to DF1 and DF2 (locations of bores and wells provided in Figure 1a). Shallow groundwater was sampled using a peristaltic pump. The groundwater wells were purged prior to sampling, and samples were collected only after conductivity and dissolved oxygen had stabilised.

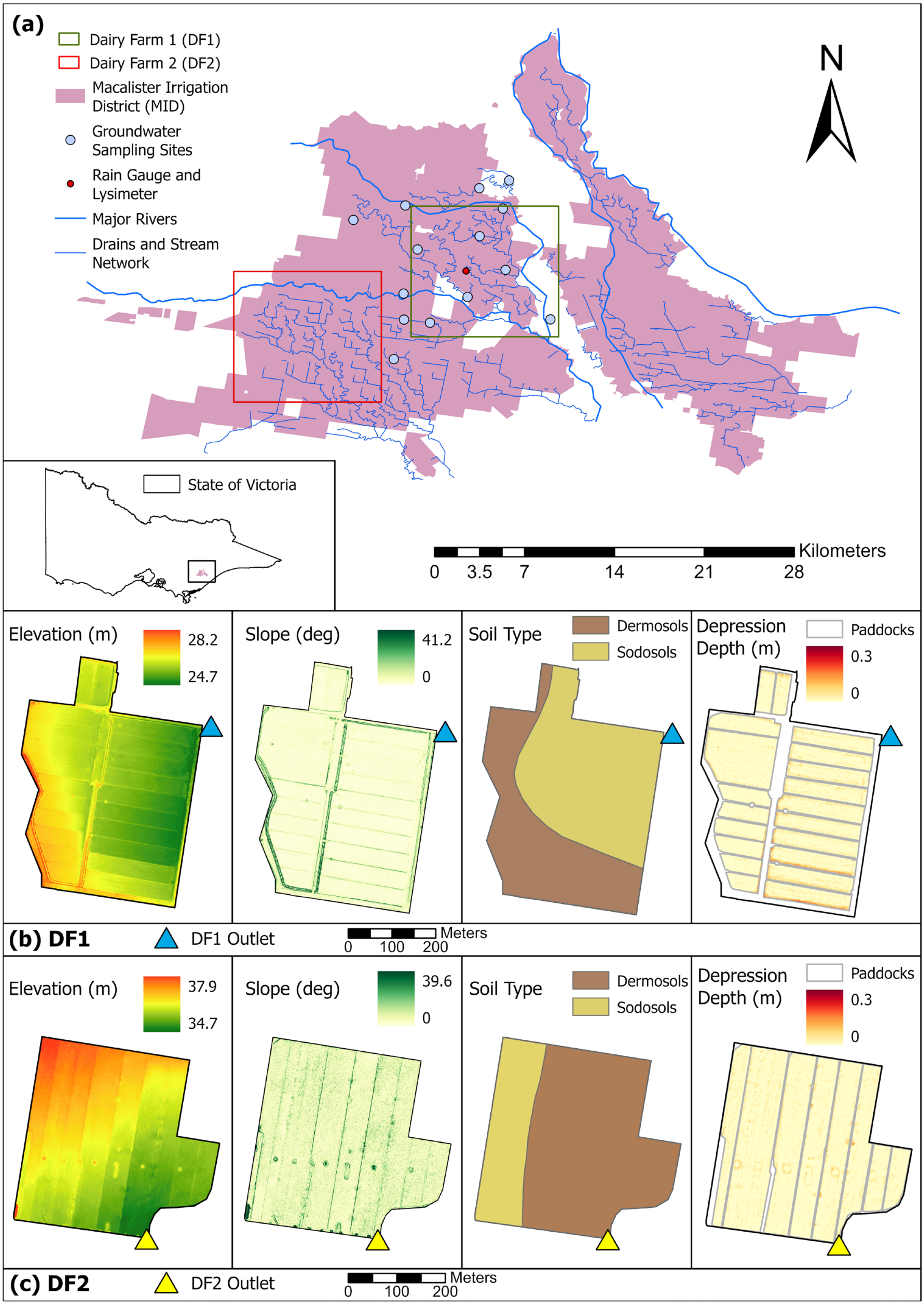

FIGURE 1 | (a) Approximate locations of Dairy Farm 1 (DF1) and Dairy Farm 2 (DF2) within the Macalister Irrigation District (MID). (b) and (c) show the elevations, slopes, soil types, and depression depths at DF1 and DF2, respectively. Exact locations of DF1 and DF2 are not shown to maintain farm anonymity.

The nutrients (nitrate (NO_3^-), nitrite (NO_2^-), phosphate (PO_4^{3-}), and ammonium (NH_4^+)) were analysed using flow injection analysis, anions sulphate (SO_4^{2-}), chloride (Cl^-), and fluoride (F^-) were analysed using ion chromatography and the cations potassium (K^+) and sodium (Na^+) were quantified using inductively coupled plasma optical emission spectroscopy (ICP-OES).

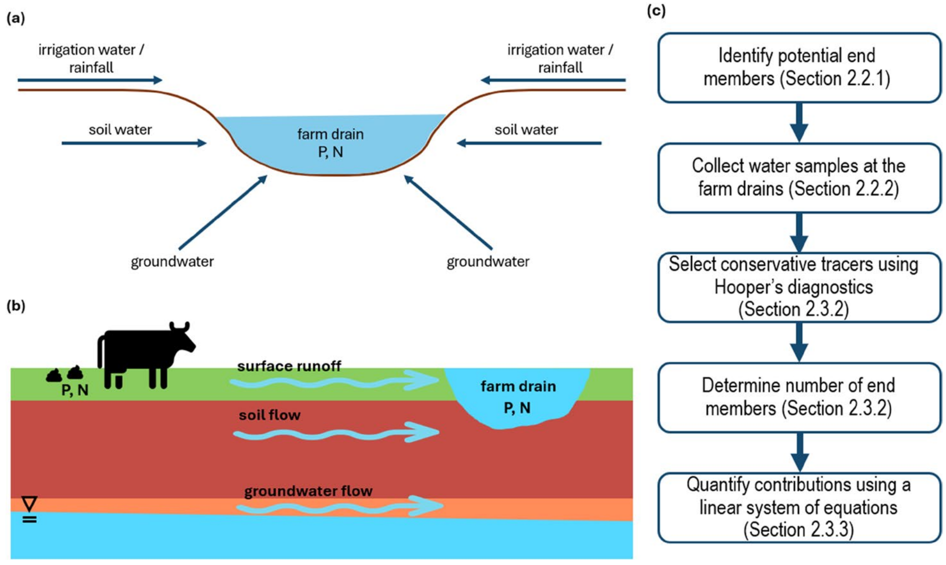

FIGURE 2 | Conceptual schematic of (a) potential end members contributing water to a farm drain which represent different (b) flow pathways of nutrients. These end members are identified and quantified via end member mixing analysis following the procedures in (c).

Rainwater, irrigation water, and groundwater samples were collected during synoptic sampling campaigns in May 2021, September 2021, and February 2022. Soil water samples were collected separately in November 2024.

2.2.2 | Measurement of Nutrients and Environmental Tracers at the Study Sites

In contrast to the end member samples, water quality at the farm drain outlets was monitored continuously between 14 December 2023 and 06 May 2024. Both DF1 and DF2 were equipped with the Eco Detection Ion-Q+ series, an autonomous, multiparameter water analysis system that monitors various water quality parameters in real-time (Eco Detection 2025). It automatically samples inorganic nutrients (nitrate (NO_3^-), nitrite (NO_2^-), ammonium (NH_4^+), phosphate (PO_4^{3-}), sulphate (SO_4^{2-})) and other ions (chloride (Cl^-), fluoride (F^-), potassium (K^+), and sodium (Na^+)) at a pre-determined frequency ranging from 1 to 6 samples per day. It analyses the samples in situ using capillary zone electrophoresis (CZE). The analysed data are transmitted to a cloud-based platform for real-time and remote monitoring.

2.2.3 | Meteorological and Hydrological Data

Rainfall was monitored using an on-site rain gauging station at DF1 which measured events at a daily timescale. At DF1, flow was measured using a pressure sensor to record water level, coupled with image velocimetry using a trail camera to estimate surface velocity (Tauro et al. 2016; Watanabe et al. 2024). The outlet structure at DF1 is a well-defined flume with a known cross-sectional profile, but subject to drowning due to downstream conditions (hence the use of image velocimetry). Flow measurements at DF2 were determined using a combination of a low-cost water level sensor (Catsamas et al. 2023) and image velocimetry. The cross-section at DF2 was lined with rubber to maintain a consistent cross-section. This cross-sectional profile was determined using a handheld LiDAR scanner.

2.3 | End Member Mixing Analysis (EMMA)

2.3.1 | Conceptual Overview

End member mixing analysis (EMMA) is based on the principle that water collected from a catchment outlet is a mixture of several distinct water sources called end members. Each end member has a distinct chemical composition defined by conservative solutes that undergo little to no reaction when the water travels through the landscape. Because only physical mixing is involved, the variations in the concentrations of the solutes will reflect the proportion of the water source. It can therefore be inferred how much of each end member contributed to the collected water sample.

To implement EMMA, end members which potentially contribute to the water sample were first identified based on prior knowledge and site observations. In the context of heavily-irrigated regions such as the Macalister Irrigation District, and particularly in the two farm drains, four potential end members were identified (see Section 2.2.1). These end members will represent flow pathways: rainwater and irrigation water will represent surface runoff, soil water will represent shallow subsurface soil flow, and groundwater will represent groundwater flow (Figure 2). In this study, we use the term "shallow subsurface soil flow" to represent a flow pathway where event water interacts strongly with the shallow soil matrix and acquires soil water chemical signatures. This term is used in a conceptual sense and does not imply the presence of a distinct lateral subsurface flow pathway typical of hillslope hydrology. The study sites provide a limited topographic gradient to support such processes (see elevation maps in Figure 1b,c). For brevity, shallow subsurface soil flow is hereafter referred to as soil flow.

After collection of environmental tracer data for the end members and farm drain samples, tracers which behaved conservatively were evaluated using diagnostic tests (details are found in Section 2.3.2). This will then allow us to calculate the contribution of each end member to the farm drains (details are found in Section 2.3.3).

2.3.2 | Determining Conservative Tracers and Number of Potential End Members

End member mixing analysis hinges on the assumption that the mixing of end members is a linear and conservative process. Conservative tracers and the number of potential end members were identified using the diagnostic approach detailed by Hooper (2003) and its quantitative extension by Liu, Bales, et al. (2008). An $n \times p$ matrix (X) of solutes was prepared, which consists of n samples of p solute concentrations. These solutes were NH_4^+, NO_3^-, PO_4^{3-}, Cl, K, Na, and SO_4. The elements of the matrix were then standardized by centering them about their means and dividing by their standard deviations, forming the standardized tracer matrix *(X*)*. This is to ensure that each tracer has an equal weight in the analysis.

Principal component analysis was performed on X^*. The orthogonal projection of X^* is given by the equation:

$$\hat{X}^* = X^* V \left(V^T V\right)^{-1} V^T \tag{1}$$

where V represents the eigenvectors corresponding to the retained principal components, and superscripts T and -1 indicate matrix operations 'transpose' and 'inverse', respectively. This projection ensures that the original tracer data is approximated in a lower dimension mixing subspace (e.g., 1-D, 2D, and 3D), while preserving the key variabilities in the tracer concentrations.

To confirm the dimensionality of the dataset, a residual analysis was performed. $\hat{X}^*$ was de-standardized to yield $\hat{X}$. The residuals (E) between the projected and original tracer matrices are given by the equation:

$$E = \hat{X} - X \tag{2}$$

Diagnostics plots were made by plotting the observed concentration for each tracer against the residuals. For each tracer, residuals were examined to determine whether they appeared to be randomly distributed. Tracers that showed no systematic structure were considered conservative. This can be done via visual inspection, as described by Hooper (2003) but was extended quantitatively by Liu, Bales, et al. (2008) to include checking metrics such as a low R^2 value, a high p value, and a low relative root mean square error (RRMSE).

The rank or dimensionality of the mixing space is determined as the lowest dimension at which residuals for the conservative tracers became approximately random. The number of potential end members of a mixture is then determined as one more than the rank of the dataset (rank + 1).

2.3.3 | Determining End Member Contributions

To determine the water sources contributing to the farm drain discharge in DF1 and DF2, as well as to quantify their relative contributions, the procedures outlined in Ali et al. (2010) were followed. A dataset was prepared containing tracer concentrations from potential end members (as described in Section 2.2.1) and farm drain samples (as described in Section 2.2.2), using only the tracers identified as conservative through the diagnostic tests outlined in Section 2.3.2. Tracer concentrations were standardized and further analysis was conducted using the correlation matrix. Principal component analysis (PCA) was performed on the dataset using the sklearn.decomposition.PCA module (Pedregosa et al. 2018) in Python and the principal component scores (PC scores) were extracted. Plotting these scores will show the locations of the end members and samples in the reduced-dimensionality space. End members were retained only if they bound the range of the samples.

To calculate the relative contributions of the end members to farm drain discharge, mass balance calculations were carried out. When two end members are retained, the contribution of each end member in the farm drain discharge can be calculated by solving the linear system of equations shown in Equations (3) and (4).

$$EM_1 + EM_2 = 1 \tag{3}$$

$$C_1 EM_1 + C_2 EM_2 = C_{fd} \tag{4}$$

where EM_1 and EM_2 are the fractional contributions of end member 1 and end member 2, respectively, while C_1, C_2, and C_{fd} are, respectively, the concentrations of the two end members and the farm drain discharge projected onto the first principal component (PC1). If more than two end members are retained, additional terms corresponding to each end member (e.g., EM_3, EM_4, and EM_5) will be added to Equations (3) and (4) as needed. Samples falling outside the domain defined by the end members, which will otherwise have values of less than 0 or greater than 1, were clipped to values of 0 and 1, respectively (Christophersen et al. 1990; Hooper et al. 1990; Liu et al. 2004).

3 | Results

3.1 | Conservative Tracers and Number of Potential End Members

To satisfy the assumptions of mixing models, tracers should behave conservatively. Figure 3 shows the residual plots that determine whether a solute behaves conservatively or otherwise. For DF1, the residual plots of Cl^-, Na^+, and K^+ showed limited structure. They consistently exhibited very low R^2 values (<0.2) and low RRMSEs ($<2\%$) across 1-D and 2-D mixing spaces. This suggests that chloride, sodium, and potassium exhibit conservative behaviour and are primarily transported through physical mixing processes instead of reactive processes within the farm paddocks. However, the three tracers had statistically significant p values ($p<0.001$) which deviate from the criterion outlined by Liu, Bales, et al. (2008), but is not unexpected considering the large sample size. In this context, the other metrics (R^2 and RRMSE) are more informative. In contrast, NH_4^+, NO_3^-, and PO_4^{3-} exhibit substantially higher R^2 values (>0.8) and larger RRMSE (7%–27%) and their residual plots show systematic patterns. SO_4 appears to be moderately non-conservative with an R^2 value of

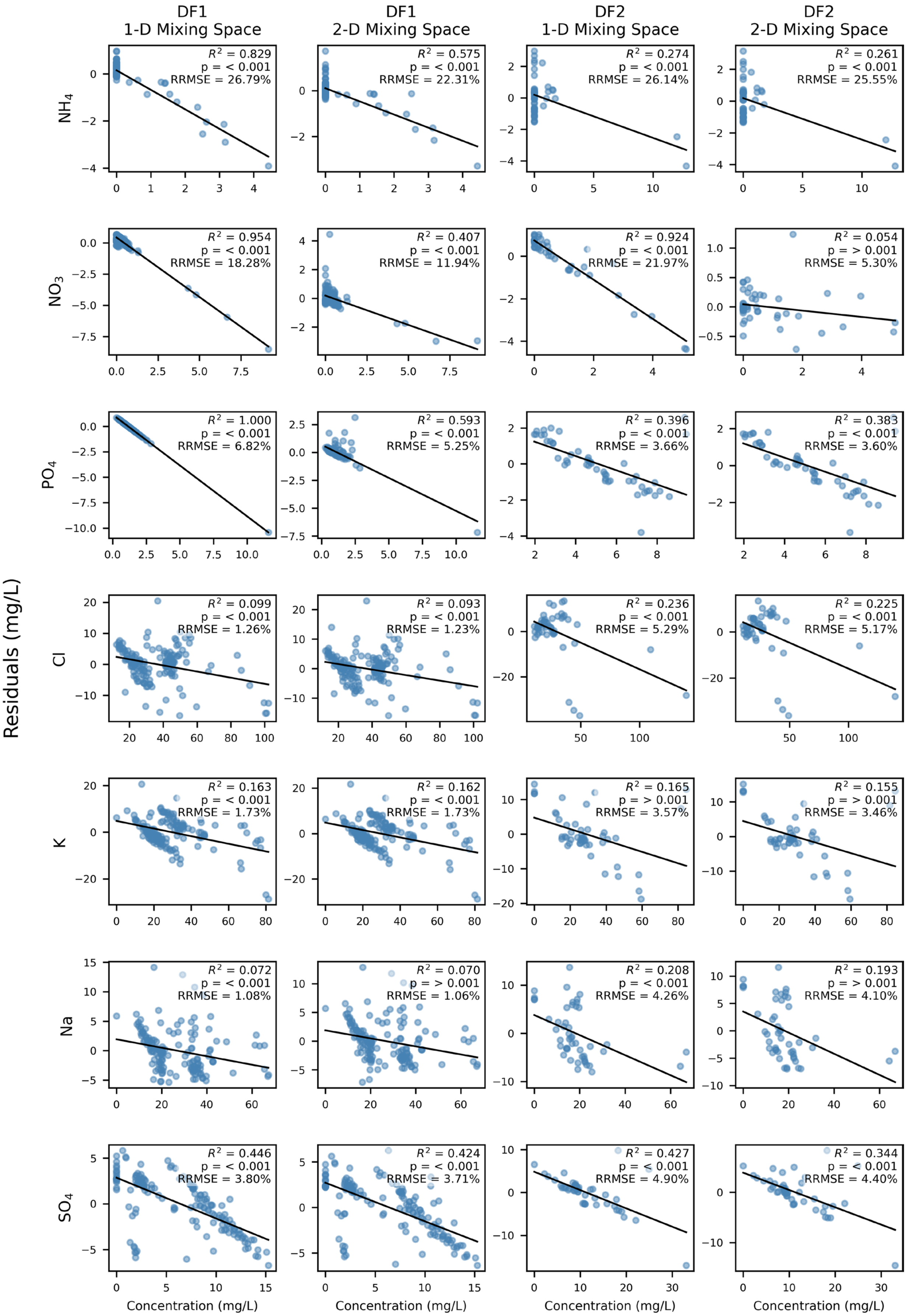

FIGURE 3 | Plots of residuals against solute concentrations observed at the farm drains under 1-D and 2-D mixing space for DF1 and DF2. R^2 and p value for slope of the regression line are also shown, in addition to RRMSE.

0.4 and RRMSE of 3.8%. These four solutes were considered to be unsuitable for defining the mixing space.

For DF2, Cl^-, Na^+, and K^+ exhibit slightly higher R^2 values (up to 0.24) and RRMSE (up to 5.3%) compared to DF1, which means that they demonstrate slightly non-conservative behaviour. Nevertheless, they remain substantially lower than those of the reactive solutes and their residual plots still lack any strong systematic trends. As demonstrated by Dendup et al. (2024), tracers that exhibit slight non-conservative behaviour can still be effectively used in EMMA, provided that their non-conservative influences are small relative to the overall mixing signal. Therefore, the conservative solutes that will be considered going forward are Cl^-, Na^+, and K^+.

At both DF1 and DF2, the 1-D mixing space appears to be sufficient to represent the dominant mixing processes of Cl^-, Na^+, and K^+. Extending to a 2-D mixing space only results in very small improvements in both R^2 and RRMSE, and the residual patterns remain generally unchanged. This means that because a 1-D mixing space is adequate, it implies that the systems at DF1 and DF2 are controlled by two dominant end members.

Eigenvector analysis further supports the adequacy of a 1-D mixing space. The first principal components at DF1 and DF2 explained 93.2% and 85.1% of the variance, respectively (Table 1). This is partly due to the fact that the selected tracers were highly collinear. Adding tracers that are not completely conservative (e.g., SO_4) may alter the dimensionality and further refine the characterization of end members. However, we prioritized conservative tracers to ensure the validity of the mixing models. Following the 'rule of 1', a principal component must explain at least 33.3% (corresponding to 1 divided by the number of tracers, i.e., 1/3) to be retained (Hooper 2003). Only the first principal component satisfies this rule. This indicates that the dataset is one-dimensional and that farm drain chemistry at both DF1 and DF2 is governed by two dominant end members.

3.2 | End Members at the Farm Drain

To determine which two end members contribute to the discharge at the monitored farm drains at DF1 and DF2, conservative tracer concentrations of potential end members were measured. Table 2 summarizes these potential end members and their ionic compositions in mg/L for Cl^-, Na^+, and K^+. The ionic compositions of these potential end members are assumed to be the same for both DF1 and DF2. Rainwater and irrigation water appear to have similar ionic compositions, specifically with their chloride concentrations (~5 mg/L). Groundwater appears to have high sodium and chloride concentrations (275 and 576 mg/L, respectively), while soil water shows intermediate values. For the case of soil water, because only one sample was able to be collected from the soil suction sampler, we included tracer concentration measurements in farm drain discharge during the recession limb of four random events. This procedure is common, as demonstrated in studies where baseflow or recession limb samples are used to represent subsurface end members, such as in (Dendup et al. 2024; Liu, Parmenter, et al. 2008). These tracer concentrations were used in the subsequent end member mixing analysis.

TABLE 1 | Explained variance and cumulative explained variance of principal components at DF1 and DF2 based on eigenvector decomposition of standardized conservative tracers (Cl^-, Na^+, and K^+).

Principal component	Explained variance (%)		Cumulative explained variance (%)	
	DF1	DF2	DF1	DF2
1	93.2	85.1	93.2	85.1
2	4.7	10.9	97.9	96.0
3	2.1	4.0	100	100

TABLE 2 | Mean ionic compositions of potential end members.

Potential end member	Cl^-	K^+	Na^+
Rainwater (4)	5.1 (3.7)	0.1 (0.1)	2.9 (2.2)
Irrigation water (6)	4.5 (3.2)	0.8 (0.2)	7.2 (2.4)
Groundwater (12)	575.7 (583)	22.6 (16.1)	275.0 (284.8)
Soil water (5)	50.2 (29.8)	57.2 (26.6)	47.1 (20.8)

Note: Conservative tracer concentrations are given in mg/L. Number in parentheses next to each end member indicates the number of samples measured. Number in parentheses next to each mean ionic concentration indicates the standard deviation.

Principal component analysis of the conservative tracer concentrations was used to define the mixing space and evaluate the contributing end members. The PCA biplots (Figure 4) of the standardized tracer data show the projections of the farm drain samples (orange dots) and potential end members (blue dots)—soil water, rainwater, irrigation water, and groundwater—in the lower dimension subspace defined by the first and second principal components. At both DF1 and DF2, the farm drain samples form a narrow, linear cluster, which confirms that the mixing space is one-dimensional.

As expected, irrigation water and rainwater are projected quite close to each other which confirms the similarity of their ionic compositions. Together, they define a common end member of the mixing space (i.e., event water end member) and represent surface runoff. Throughout the manuscript, we refer to the term "event water" when distinction between rainwater and irrigation water is not required.

Soil water is shown towards the opposite end of the mixing space, distinct from event water at both DF1 and DF2. It exhibits high variability along PC2 (as indicated by a large spread along this direction) but appears to be well constrained along PC1. This shows that soil water is not a single fixed composition but can vary spatially and temporally and represents a range of subsurface conditions. With soil water on one end and event water on the other end bounding the farm drain samples, a one-dimensional mixing space is confirmed, as we have previously established in Section 3.1. In contrast, groundwater is located far from the farm drain samples and the other end members

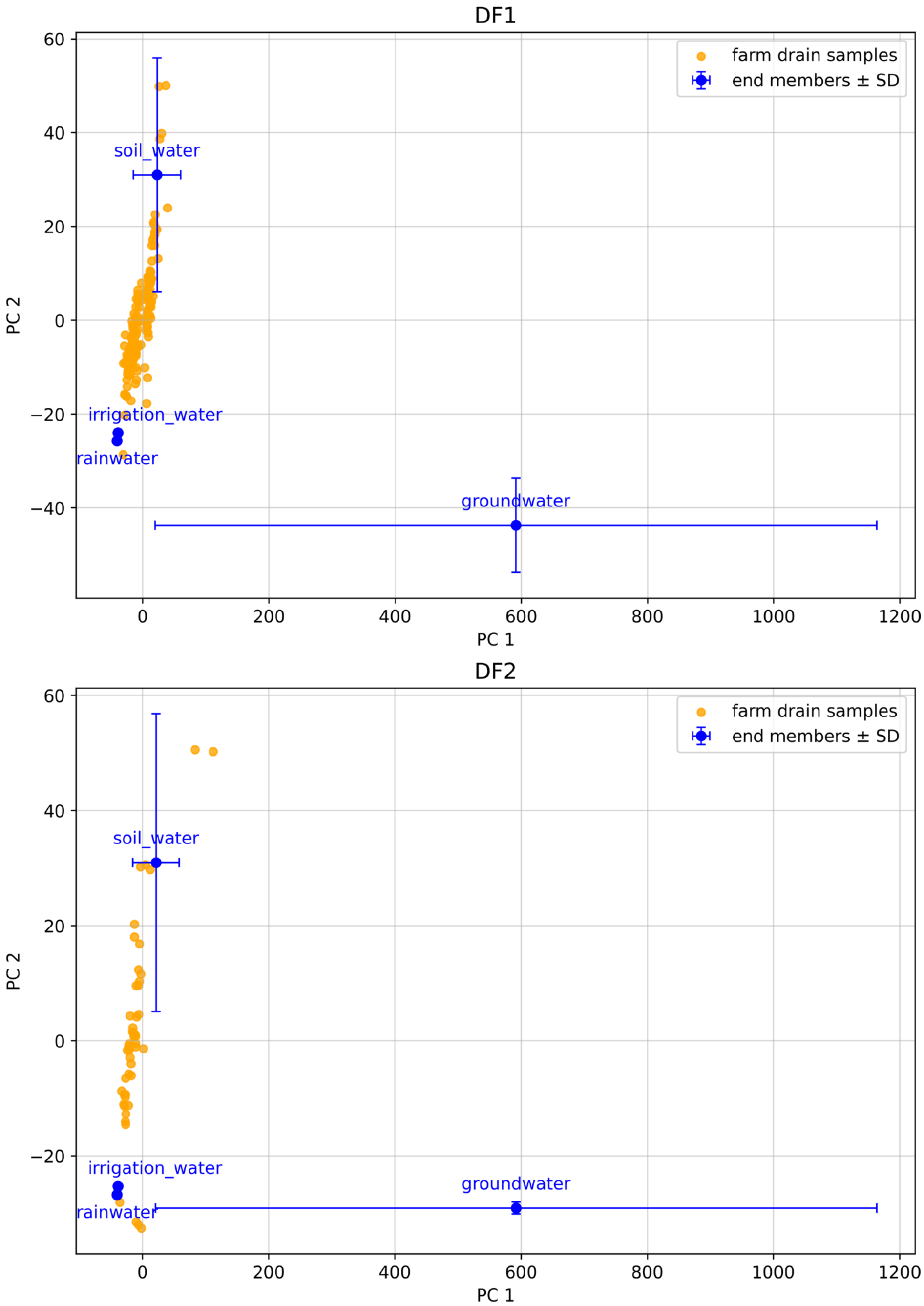

FIGURE 4 | Principal component analysis (PCA) of conservative tracers (Cl^-, Na^+, and K^+) from farm drain samples (orange dots) and potential end members (blue dots) at DF1 and DF2 projected onto a lower-dimensional mixing space composed of the first two principal components (PC1 and PC2). Soil water, irrigation water, and rainwater bound the farm drain samples while groundwater shows distinct tracer signatures, suggesting that farm drain discharge is a linear mixture between soil water and irrigation water during irrigation events and soil water and rainwater during rainfall events.

in the mixing space, which indicates a distinct ionic composition. This indicates that there is a very limited contribution of groundwater to the farm drain discharge at both sites during the monitored events. There is also a large spread associated with groundwater along PC1, which means that we cannot definitively exclude minor contributions. However, the alignment of the farm drain samples along the 1-D mixing space between soil water and event water shows that these end members dominate the observed variability in farm drain chemistry during the monitored events.

In summary, the results indicate that farm drain water chemistry is primarily a mixture of soil water and rainwater during rainfall events, and soil water and irrigation water during irrigation events (which, in the Australian context, usually occur under dry conditions with no concurrent rainfall), with limited influence from groundwater based on the selected conservative tracers. This shows the dominance of surface runoff and soil flow contributing to drain discharge. The limited influence of groundwater suggests that deep subsurface flow pathways are hydrologically disconnected from these two farms. Similar disconnections may also occur in other parts of the Macalister Irrigation District. Further investigation across a larger number of farms would be required to assess whether this disconnection between the farm drains and groundwater is representative of the district as a whole.

3.3 | Hydrologic Controls and Flow Response

Nine hydrologic events were observed at DF1 between December 2023 to April 2024 (Figure 5a). Three of these events were rainfall-driven (December and January), while the other six were irrigation-driven (February to April). One rainfall event in January 2024 lacked nutrient/solute measurements and was excluded from further analyses. Rainfall volumes (25 and 35 mm) were substantially smaller compared to irrigation inputs (60 mm–130 mm). The resulting peak discharges for the two rainfall events are only around 0.131 mm/h and 0.075 mm/h, while the irrigation events had peak discharges of at least 0.187 mm/h to as high as 0.317 mm/h. No discharge is observed in between events, which shows that flow from the farm drain is event-driven and suggests that there is no groundwater contribution to sustain baseflow.

At DF2, six events were recorded (Figure 6a). Four of these events were rainfall events while the other two were irrigation events. Three rainfall events (in December and January) produced relatively small discharge responses (0.025–0.130 mm/h). One rainfall event in April with a total volume of 33 mm produced a hydrograph which peaked at 0.450 mm/h. Irrigation inputs data at DF2 were not available. However, we can infer that any runoff occurring in the absence of any recorded rainfall is driven by irrigation inputs. Similar to DF1, the discharge peaks during these events are also higher compared to the rainfall-driven discharge peaks at 0.670 and 0.700 mm/h, which are almost double the peak discharge of rainfall events.

3.4 | End Member Dominance During Rainfall and Irrigation Events

There is a stark contrast in end member dominance during rainfall versus irrigation events at DF1 (Figure 5b). For the two rainfall events in December 2023 not exceeding 35 mm, the runoff at the farm drain is dominated by soil water (> 90% soil water at each sample time). Irrigation-driven events at DF1, in contrast, show the dominance of irrigation water inputs comprising approximately 60%–80% of the total discharge volume. This was expected since irrigation inputs were more than approximately twice the magnitude of rainfall inputs. Irrigation water contributions were highest during the rising limb and peak flow, with fractions reaching ~70% at the hydrograph peak. The contribution of soil water then begins to increase during the recession limb.

During rainfall events at DF2, we see different end member behaviour compared to those at DF1 despite roughly similar input volumes (Figure 6b). While farm drain water during rainfall events at DF1 was dominated by soil water, farm drain water at DF2 was dominated by rainwater. Additionally, the three succeeding rainfall events from December to January that are approximately 1 week apart show increasing fractions of rainwater. Only two irrigation events were observed during the measurement period at DF2. The first irrigation event in February behaved similarly to DF1, where irrigation water was dominant, particularly at the hydrograph peak. The second irrigation event took place in mid-March, approximately 45 days after the previous application. The dominant end member during this event on average was soil water, although soil water and irrigation water contributed approximately equal proportions around the hydrograph peak. This behaviour contrasts with that of DF1, where irrigation was consistently dominant across all irrigation events.

3.5 | Reactive and Conservative Nutrient Export Trends

There is a variable trend in instantaneous loads of reactive nutrients (PO_4^{3-}, NO_2^-, NO_3^-, and NH_4^+) exported to the farm drains across different events at DF1 (Figure 5c–e). Instantaneous loads are presented here to describe the timing and relative magnitude of nutrient export during rainfall and irrigation events (concentration timeseries are shown in Figures S4 and S5).

Ammonium loads (Figure 5e) increased during the first rainfall event in December (~10.5 mg/s or ~0.05 kg/ha/d) and in the first irrigation event in February (~26.2 mg/s or ~0.12 kg/ha/d), likely due to the availability of NH_4^+ from manure present on the paddock surface. Subsequent events after these spikes showed little to no NH_4^+ loads, potentially due to the depletion of available sources or its transformation via volatilization and nitrification (Ma et al. 2010; Norton and Ouyang 2019; Tian et al. 2021).

Nitrate export differed between rainfall and irrigation events (Figure 5d). For the two rainfall events, no NO_3^- loads were detected. Farm drain discharge during these two events is dominated by soil flow (Figure 5b). In contrast, instantaneous NO_3^- loads reached as high as ~100 mg/s (or ~0.45 kg/ha/d) at the start of the first irrigation event (when irrigation water is dominant) and decreased in subsequent events to around 20–40 mg/s (or 0.09–0.18 kg/ha/d). This relatively high spike during the irrigation event in February, which is the first irrigation event observed during the monitoring period (summer in the Australia context), may be due to the accumulation of mineralized organic matter and manure, as well as residual fertilizer from past applications.

Loads of SO_4^{2-}, Cl^-, Na^+, and K^+ varied with discharge, increasing during the rising limb and decreasing during the recession limb of the hydrograph (Figure 5f–j). This pattern is consistent across events, with no apparent distinction between rainfall-driven or irrigation-driven events. Phosphate (PO_4^{3-}) loads also increased with discharge; however, PO_4^{3-} concentration trends (see Figure S4) were different from the conservative tracers, which indicates that availability is controlled by biogeochemical processes. During high flow events, physical transport processes dominate, as overland flow likely mobilises and transports both dissolved and particulate phosphorus from the soil surface.

The solute export patterns at DF2 (Figure 6c–j) were broadly similar to those at DF1. Irrigation events still produced the largest instantaneous loads with pronounced spikes in NO_2^-, NO_3^-, NH_4^+,

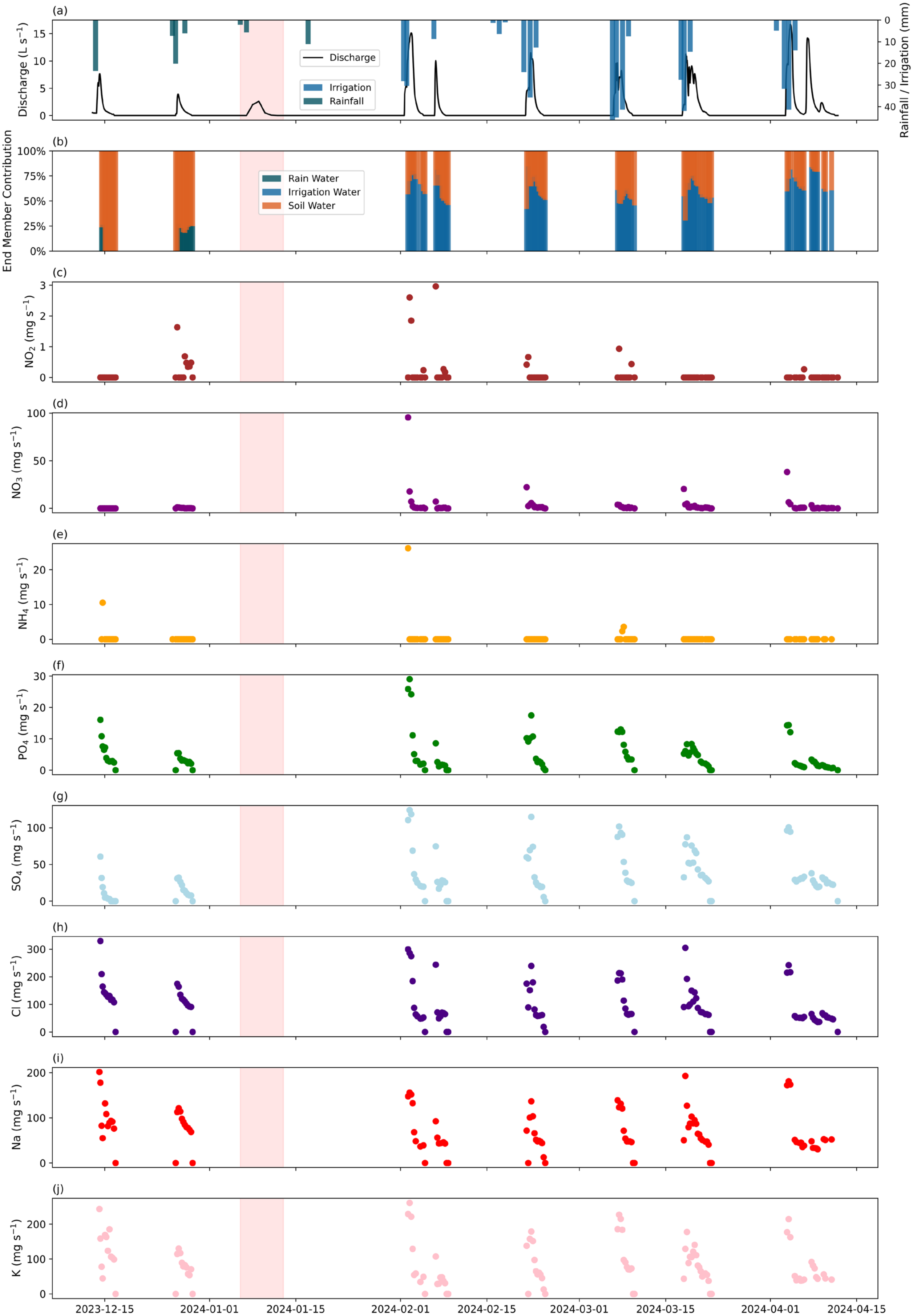

FIGURE 5 | Legend on next page.

FIGURE 5 | Time series of (a) discharge, rainfall, and irrigation inputs; (b) end member contributions; and (c–j) nutrient/solute loads (reported in mg/s) in farm drain water at DF1. No nutrient/solute measurements were made during the rainfall event and subsequent discharge on January 06–11, 2024, as highlighted with the red box.

and PO_4^{3-}. Rainfall events yielded small nutrient loads, with only small spikes in NO_3^- and PO_4^{3-}, and little to no NH_4^+. Conservative solute loads such as SO_4^{2-}, Cl^-, Na^+, and K^+ increased and receded together with discharge regardless of event type. Overall, solute loads at DF2 showed similar hydrology-driven export trends as DF1.

3.6 | Dominant Flow Pathways of Nutrients Across Events

Across DF1 and DF2, two contrasting nutrient load export behaviours were observed between irrigation-driven and rainfall-driven events, but with differences in the dominant end members (Figures 7 and 8). Each nutrient is expressed as a ratio to chloride so that dilution and enrichment effects caused by variations in discharge are normalised.

At DF1, rainfall events (Figure 7a,b) were dominated by soil water (> 90% of the total discharge volume (panel ii)). The nutrient: Cl^- ratios appear to remain nearly constant at very low values (< 0.05). In contrast, irrigation events (Figure 7c,d) were dominated by irrigation water (70%–80% contribution). The NO_3^-:Cl^- ratio in Figure 7c immediately increased to 0.32 at the beginning of the event and declined thereafter. Similar but smaller initial spikes were observed for NH_4^+ and PO_4^3.

At DF2, rainfall events (Figure 8a,b) were dominated by rainwater and the nutrient:Cl^- ratios showed early event increases which resemble those of the irrigation events at DF1. During irrigation events at DF2 (Figure 8c,d) when soil water contributions were higher, NO_3^-:Cl^- and NH_4^+:Cl^- ratios remained low (< 0.07). Nitrate was more dominant than ammonium (Figure 8c,d) but only by a very small fraction (0.05).

4 | Discussion

4.1 | The Role of Microtopography, Surface Roughness, and Antecedent Moisture Conditions in Controlling End Member Contributions

Our results have shown contrasting patterns in end member dominance observed at DF1 and DF2 and these can likely be explained by microtopography, surface roughness, and antecedent soil moisture conditions. At DF1, rainfall events were dominated by soil water. This suggests that there is strong interaction between runoff and the shallow soil matrix. Several mechanisms may explain this behaviour. One potential explanation is that water fully infiltrated into the soil and was followed by lateral subsurface flow and exfiltration at the farm drain (Figure 9a). However, there is little elevation gradient to drive this subsurface flow, and in the absence of clear evidence of a strong hydraulic gradient or a restrictive soil layer, it is therefore unlikely to occur in the DF1 study site. A second possible explanation is that pure diffusion of solutes from the soil is occurring (Figure 9b). However, this process can take weeks to occur and is therefore unlikely to influence event-scale hydrochemistry.

A third possibility, which we consider the most plausible mechanistic explanation, is that overland flow undergoes repeated small-scale infiltration and exfiltration driven by microtopographic roughness (Figure 9c). This roughness slows the flow and allows for exchanges between event water and the shallow soil matrix. This interpretation aligns with the conceptual framework of Oldham et al. (2013), where slower water movement increases exposure time and therefore the extent of exchange between water and its surrounding medium.

Some numerical and remote sensing experiments have shown that microtopographic depressions can act as transient storage zones and govern the degree of hydrologic connectivity across a paddock or field (Appels et al. 2011, 2016; Ghimire et al. 2021). Even small depressions and surface roughness elements can delay overland flow, increase residence times, and promote repeated infiltration-exfiltration between runoff and the shallow soil. Some overland flow models by Abbasi et al. (2003) have likewise shown that other surface roughness features such as wheel tracks, pasture tussocks, and animal paths can cause lateral resistance, modulate velocities, and enhance solute exchange. For the case of the rainfall events at DF1, the relatively low input volumes (25–35 mm) were likely not sufficient to overcome these roughness features delaying overland flow and allowing event water to equilibrate with soil water.

The opposite is true during irrigation events at DF1 when the relatively high irrigation inputs (60–130 mm) are applied onto the paddocks. We see the dominance of irrigation water during these irrigation events. In flood irrigation, high rates and volumes of water input exceed the infiltration capacity of the soil, causing overland flow to propagate water down the irrigation bay and water the whole field. This would have caused microtopographic depressions across the paddocks to 'fill and spill' which would have allowed for efficient hydrologic connectivity between the irrigation source and the monitoring drain via surface flow pathways.

At DF2, rainfall events were dominated by rainwater, which suggests that there was reduced interaction between rainwater and the shallow soil matrix compared to DF1. This contrast may be a result of the differences in the surface microtopography between the two study sites. Such differences are visually evident in the depression depth map of DF1 and DF2 found in Figure 1b,c, respectively. These maps were derived from raster analyses of a 0.5-m resolution digital elevation model (State of Victoria Department of Transformation and Planning 2025) (see Supporting Information Section S2). DF2 shows shallower microtopographic depressions than DF1 and a lower total depression storage (~7.9 mm compared to 12.3 mm at DF1). With these shallower local depressions, it is likely that rainwater can more

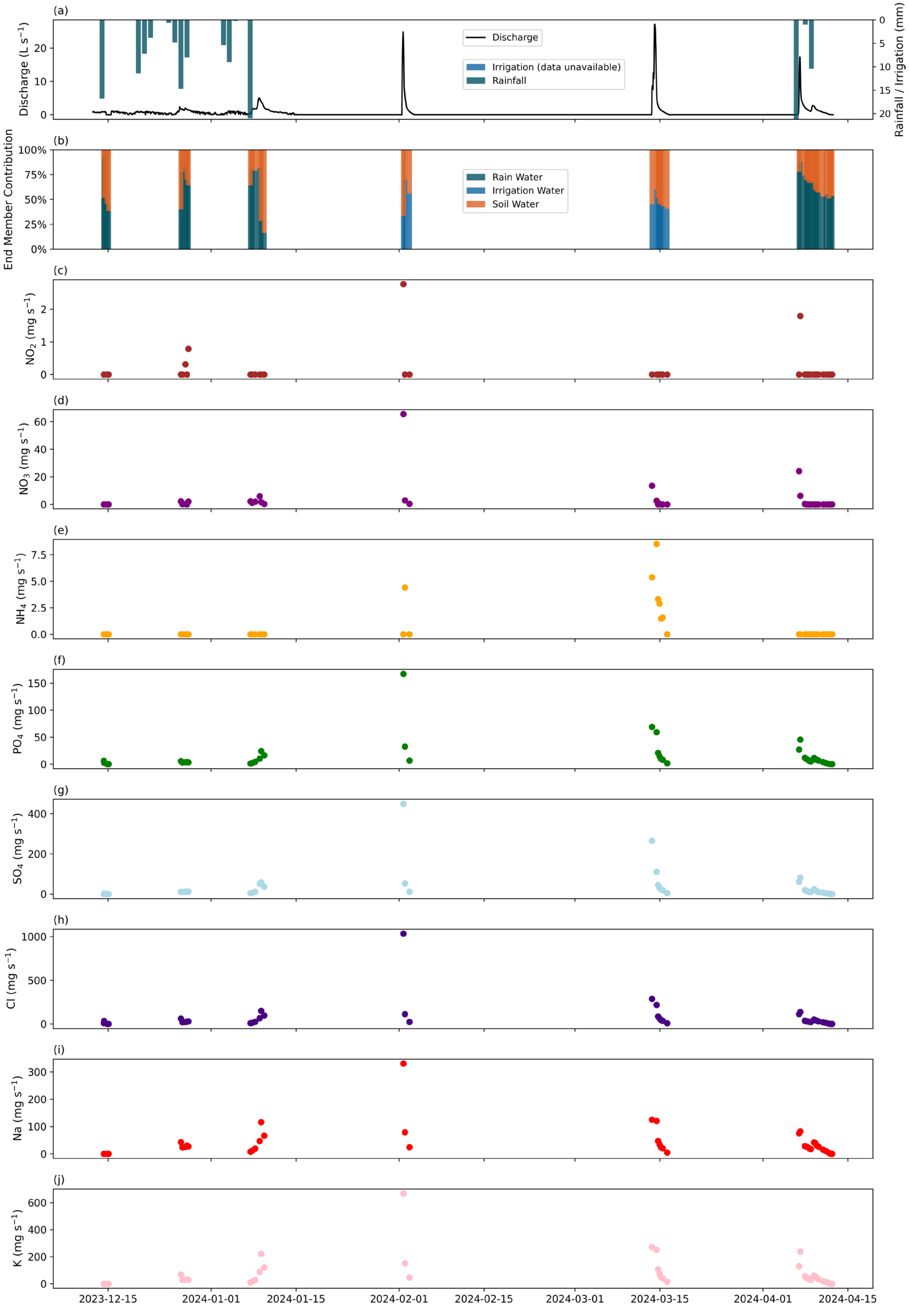

FIGURE 6 | Legend on next page.

FIGURE 6 | Time series of (a) discharge, rainfall, and irrigation inputs; (b) end member contributions; and (c–j) nutrient/solute loads (reported in mg/s) in farm drain water at DF2. Irrigation volume data were not available but can be inferred as the hydrological input where discharge was recorded without concurrent rainfall.

quickly generate overland flow, which would allow a larger fraction of the rainwater to reach the farm drain. Consequently, there would be a reduced opportunity for the rainwater to equilibrate with soil water via local infiltration-exfiltration, resulting in rainwater being the dominant end member at the outlet.

Previous field studies have shown that compaction from cattle grazing and treading increases soil bulk density and reduces macropores. This decreases infiltration capacity and therefore promotes surface runoff generation (Franzluebbers et al. 2012; Gray et al. 2022). Findings by McDowell et al. (2003) complement this with their observation that trampling-induced reductions in macroporosity substantially shortened the time to initiate runoff and increase overland flow volumes.

Another contrasting observation at DF2 is that soil water is dominant during an irrigation event after a prolonged dry period (~45 days). This extended dry period possibly increased the soil moisture deficit and increased the soil's capacity to store water. Soil surface crusting during this period was unlikely due to good vegetation cover and the observed response suggests that infiltration remained sufficient. When the irrigation water was applied, much of the applied water infiltrated to replenish the depleted storage. Even though DF2 has shown rapid runoff generation in most events, the prolonged dry period likely increased soil moisture deficit such that infiltration initially replenishing soil storage first appears to have delayed overland flow, and the greater infiltration would have led to more soil interactions. This shows how antecedent moisture conditions can influence which dominant end member reaches the farm drains.

4.2 | Surface Runoff Drive P and N Export

Our findings provided evidence that nitrate is mobilized via surface runoff under flood irrigation or rainfall, and we hypothesise that this occurs on heavily compacted soils. The immediate spike in the NO_3^-:Cl^- ratio at the beginning of an irrigation event suggests that there is a ready pool of NO_3^- at the soil surface that gets mobilized and transported to the farm drains. This nitrate likely comes from sources such as residual fertilizer (applied urea that has transformed to nitrate) and manure (Murphy et al. 2024; Sądej and Przekwas 2008). Specifically, organic nitrogen is first mineralized into NH_4^+ which is then transformed via volatilization and nitrification. These are possible because irrigation in our study area occurs every 11–15 days which allows for warm and aerobic conditions to occur in between events. Volatilization and nitrification can be completed within 3 days to 2 weeks or longer (Ma et al. 2010; Norton and Ouyang 2019; Tian et al. 2021). This also explains why there is barely any NH_4^+: Cl^- spike in our results for the two irrigation events, because most, if not all, of the NH_4^+ may have been volatilized and/or nitrified to NO_3^- prior to irrigation.

Our findings that nitrate is exported via surface runoff contrast numerous studies that found the dominant pathway of nitrate to be via subsurface flow in both catchment-scale and farm-scale studies. For instance, nitrate was reported to be delivered primarily through shallow groundwater flow in a North Carolina catchment, moving through saturated zones with minimal denitrification (Tesoriero et al. 2005). Similarly, in humid, tropical catchments where sugarcane is cultivated, nitrate was exported laterally through shallow groundwater flow into creeks, accounting for more than 50% of the total nitrogen loads (Rasiah et al. 2013). At a smaller scale, in an intensively managed dairy farm, nitrate export mainly occurred through tile drains and lateral subsurface flow (Fenton et al. 2022). Even in a small, experimental loess soil plot-scale study under simulated rainfall, nitrate was shown to have a deeper effective depth (~9–11 cm) and was transported through infiltration (Zhang and Zhang 2009). In contrast, despite contributions of soil water to discharge in our study sites, it appears to be relatively low in NO_3^-, suggesting that the dominant nitrate sources in these systems are more readily available on the surface and are therefore more effectively mobilized via surface runoff. Water that deeply infiltrated into the soil profile may possibly mobilize nitrate towards the regional groundwater which lies below the level of the surface drainage system.

Our study sites have different conditions from the aforementioned studies. We hypothesise that irrigation inputs at DF1 were large enough to overcome surface roughness features, while compaction from grazing at DF2 relatively smoothened surface roughness. These conditions allowed for the rapid generation of overland flow which then mobilised readily available nitrate and phosphate on the surface. In addition, the relatively small spatial extent of the study paddocks meant that the runoff quickly reaches the farm drains. This allows limited opportunity for percolation. This contrasts with catchment-scale studies where a longer flow path means there is potential for water to infiltrate as it travels downstream. In fact, a study of 22 catchments in the Western Lake Erie area found that surface water transporting nitrate initially travels via surface pathways, but an increase in the drainage area would lengthen the travel of surface runoff and therefore allow for reinfiltration into the soil, contributing nitrate to subsurface flow (Song et al. 2022).

4.3 | High Nutrient Exports due to Flood Irrigation

High loads of nutrients were exported during irrigation events at DF1 (as high as 0.450 kg/ha/d of NO_3^-, 0.134 kg/ha/d of NH_4^+, and 0.134 kg/ha/d of PO_4^{3-}) and DF2 (as high as 0.390 kg/ha/d of NO_3^-, 0.045 kg/ha/d of NH_4^+, and 0.960 kg/ha/d of PO_4^{3-}) compared to rainfall events at both farms (no loads detected for NO_3^-, 0.045 kg/ha/d of NH_4^+, and 0.080 kg/ha/d of PO_4^{3-} at DF1 and no loads detected for $NO_3^-$and and 0.300 kg/ha/d of PO_4^{3-} at DF2). Excess water from flood irrigation flows across the paddock surface, mobilizing and transporting nutrients that accumulated on the soil surface to the farm drains. Surface runoff was dominant during these events as evidenced by the dominance

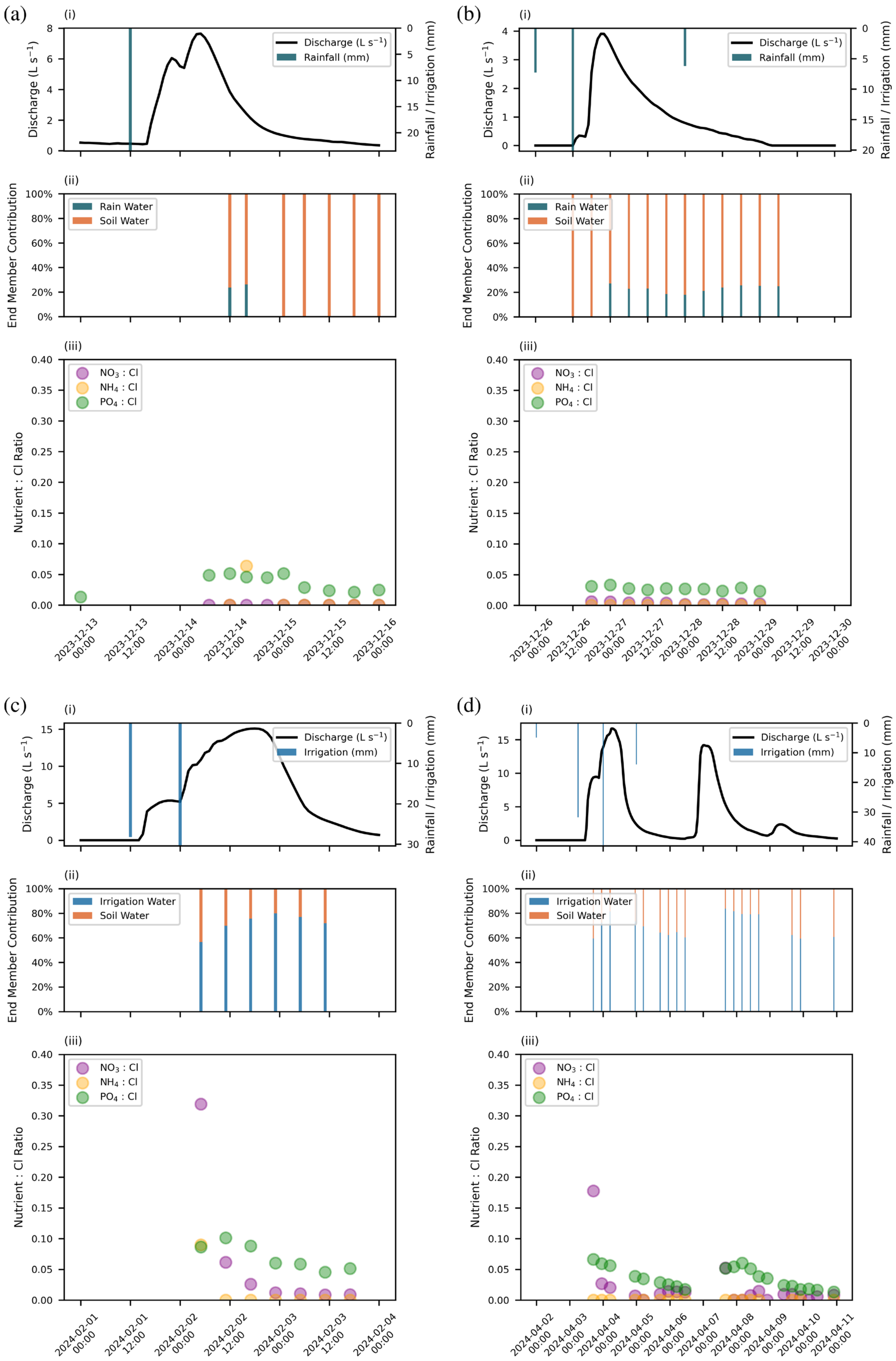

FIGURE 7 | Legend on next page.

FIGURE 7 | Time series of (i) discharge and rainfall or irrigation inputs, (ii) end member contributions, and (iii) mass-based nutrient-chloride ratios for (a and b) two rainfall events and (c and d) two irrigation events at DF1. Each nutrient is expressed as a ratio to chloride so that dilution and concentration effects caused by variations in discharge are normalised. Two contrasting nutrient-export behaviours can be observed between rainfall and irrigation events.

of irrigation water sources identified from end member mixing analysis. These findings are consistent with studies which have shown the nutrient export from irrigated dairy pastures (Mundy et al. 2003; Nash et al. 2007) is relatively higher than those from non-irrigated/rainfed dairy pastures (Fleming et al. 2001; Holz 2010). For instance, Barlow et al. (2007) measured as high as 58 mg/L of mean annual total nitrogen (TN) in runoff from an irrigated dairy pasture compared to 29 mg/L from a rainfed dairy pasture. Additional case studies from Australia and New Zealand show that flood-irrigated fields export 2 to 4 times more total N and P compared to neighbouring spray-irrigated systems (Wilcock et al. 2011).

The nutrient loads observed during irrigation events showed a first-flush pattern wherein the nutrient:Cl^- ratios peaked almost immediately at the start of the irrigation event, along the rising limb of the hydrograph. This is similar to the observations made in a small agroforest catchment where the rise in the concentration of P coincided with the rising limb and peak of the hydrograph (Luz Rodríguez-Blanco et al. 2009), as well as farm-scale studies that observed high P concentrations during early stages of surface runoff from areas with recent manure depositions such as barnyards, cattle paths, roadways, and grazed paddocks (Fenton et al. 2022; Hively et al. 2005; Holz 2010; McGechan et al. 2005). Phosphorus in our study area likely comes from a combination of soil P derived from historical fertilizer inputs and cow manure deposited on the paddocks, all of which are susceptible to mobilization via surface runoff during flood irrigation events. The dominance of surface runoff for phosphorus mobilization also help explain the relatively high concentrations of phosphorus (3–30 mg/L) in runoff from the Macalister Irrigation District (Barlow et al. 2006; Nash et al. 2005). One would expect sorption to soil (Casey et al. 2001) to moderate phosphorus concentrations if subsurface flow pathways were significant.

4.4 | Study Limitations and Directions for Future Research

Our study presents insights into nutrient transport dynamics under flood irrigation, but some limitations must be acknowledged. Firstly, the monitoring period was relatively short (~4 months during most of the summer period) and captured only a small number of hydrological events. This limits our ability to fully characterise seasonal variability of nutrient export. In addition, the findings of this study should be interpreted within the context of flood-irrigated systems since comparison across other irrigation systems was not conducted. Future research should extend the monitoring period to at least a one-year cycle or more to capture a wider range of events and across different irrigation systems.

Despite these limitations, our study offers insights into nutrient dynamics under low-intensity rainfall and flood irrigation. The consistent patterns in our key findings provide confidence in the robustness of our interpretations. This study provides insights that could serve as foundations for further studies, as well as for planning effective farm-scale nutrient export interventions.

4.5 | Implications for Farm-Scale Management

Our finding that surface runoff dominates nutrient transport off irrigated dairy farms has several implications for management of similar irrigated dairy farms. Our findings indicate that frequent irrigation is likely to increase the risk of mobilization and transport of phosphorus and nitrate. Reducing the frequency of irrigation and adopting deficit irrigation strategies, which is when water is applied only when soil moisture levels fall below a threshold, may be a way to mitigate this process. Using APSIM modelling of overhead spray irrigation systems, Vogeler et al. (2019) found that maintaining large soil moisture deficits did not compromise pasture yield but significantly reduced nitrogen losses. When economically feasible, upgrading to a more controlled irrigation system such as pivot or spray irrigation can reduce nutrient export. This is because these systems produce lower runoff volumes compared to flood irrigation methods (Monaghan et al. 2009).

The importance of the 'first flush' in nutrient exports suggests that management interventions that capture surface runoff, such as recycling or reuse dams, may be particularly effective in reducing nutrient losses from heavily-irrigated dairy systems. These structures can reduce direct hydrologic connectivity between the paddocks and the farm drains and capture irrigation tailwater or rainfall and early event runoff when nutrient concentrations and loads are highest. Proper management of reuse structures is also critical. Given that nutrient export in this study was observed to be driven by hydrologic events, maintaining relatively high water levels in reuse systems increases the risk of spills (Finger et al. 2018). Low water levels must be maintained prior to irrigation or forecasted rainfall events to ensure that nutrient-rich early event runoff is captured.

In addition to irrigation and reuse systems, maintaining surface roughness may further reduce rapid surface runoff and the nutrients that come along with it. In practice, this can be achieved through management practices such as maintaining pasture cover, increasing biomass, and minimizing soil compaction from livestock traffic. While microtopographic depressions can also attenuate rapid runoff, such features often minimise irrigation water use efficiency and increase the risk of salinization. Practices that enhance roughness without substantially increasing depressions offer a balance between water use efficiency and nutrient transport mitigation. These measures can complement other flow attenuation measures such as the previously discussed reuse systems.

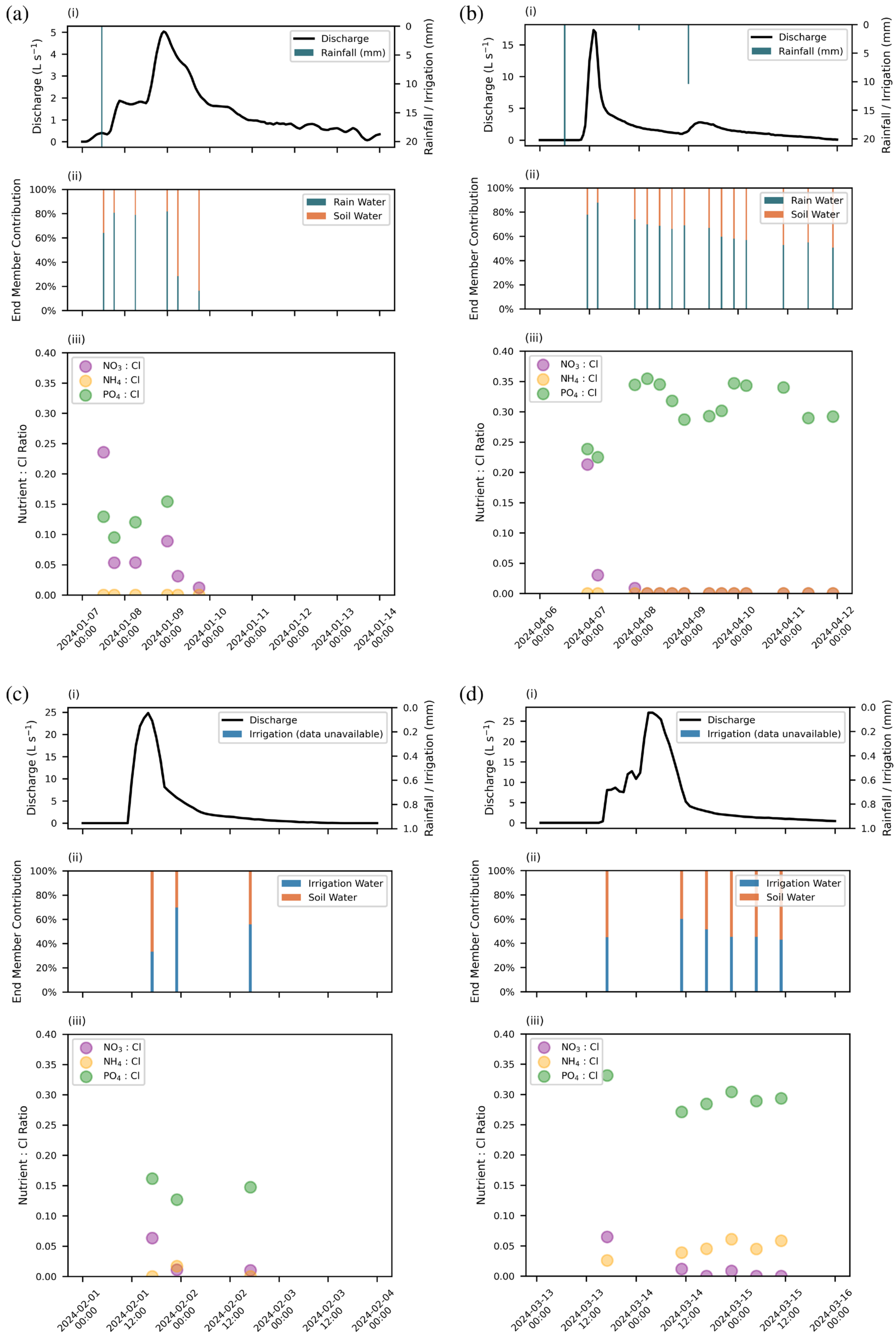

FIGURE 8 | Legend on next page.

FIGURE 8 | Time series of (i) discharge and rainfall or irrigation inputs, (ii) end member contributions, and (iii) mass-based nutrient-chloride ratios for (a and b) two rainfall events and (c and d) two irrigation events at DF2. Irrigation volume data at DF2 (for panels c and d) were not available but can be inferred as the hydrological input where discharge was recorded without concurrent rainfall.

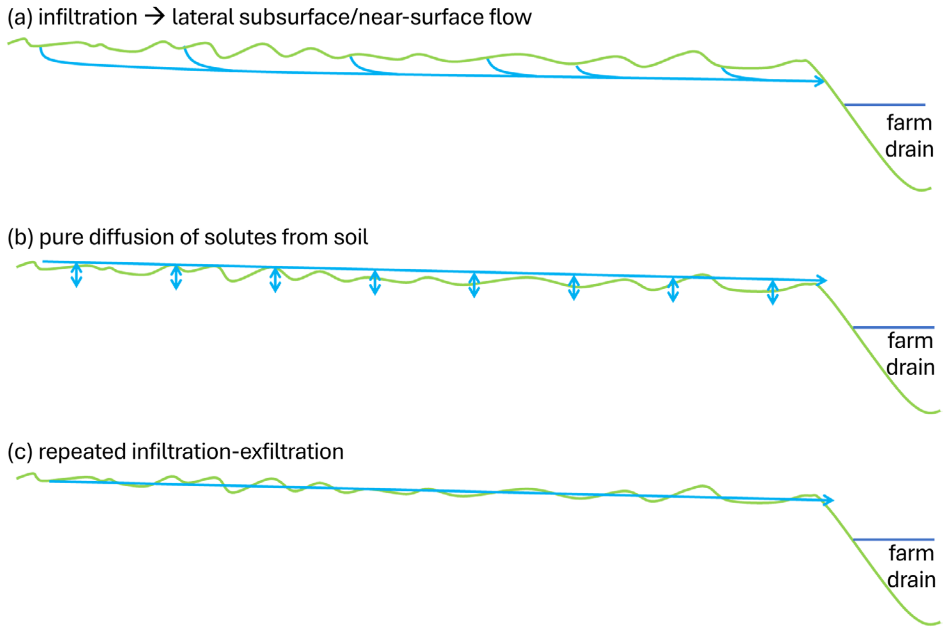

FIGURE 9 | Plausible mechanisms for how event water acquires soil water chemical signatures to explain the dominance of soil water fractions at the farm drains during rainfall events at DF1: (a) infiltration followed by lateral subsurface flow, (b) pure diffusion of solutes from soil, and (c) repeated infiltration-exfiltration driven by microtopographic roughness (most plausible at DF1).

5 | Conclusions

Our study applied end member mixing analysis (EMMA) to determine the dominant hydrologic pathways and their role in exporting nutrients from two flood-irrigated dairy farms in the Macalister Irrigation District, Victoria, Australia. Using this technique, we were able to differentiate between three water sources: irrigation water and rainwater (which represent surface runoff) and soil water (which represents soil flow). The results consistently showed that surface runoff was the dominant pathway of nutrient transport, with surface runoff dominating in 70%–80% of events.

Differences in end member dominance (water source) between farms are likely controlled by surface roughness, microtopography, and antecedent soil moisture conditions. At DF1 where there was greater microtopographic storage, the dominant end member during low-intensity rainfall events was soil water. In contrast, at DF2, reduced surface roughness and shallower depressions allowed for faster overland connectivity and rapid overland surface routing, and a greater contribution of rainwater. During irrigation events, large water inputs rapidly filled surface depressions promoting immediate hydrologic connectivity, which is why there appears to be little variation in contributions between farms (except when there is an antecedent dry period, where event/irrigation water contribution decreases for one of the farms).

Coupling EMMA with nutrient-to-chloride ratios revealed that nitrate and phosphate have a pronounced "first flush" behaviour during events when surface runoff is dominant. In contrast, events when soil flow was dominant are associated with low nutrient export.

In summary, surface runoff is the primary driver of nutrient export from flood-irrigated dairy systems. Management strategies that reduce the magnitude or frequency of surface runoff include deficit irrigation, use of sprinkler irrigation systems, adoption of reuse systems and their effective operation, and preservation of surface roughness and microtopography. The importance of surface runoff also explains the high phosphorus export from the district, which highlights the need for effective manure management.

Acknowledgements

We wish to thank our partner farmers for allowing us to monitor their dairy farms. We are grateful to Jasmine Kneebone for providing us with a comprehensive paddock rotation schedule and detailed irrigation volume data at DF1. We thank EcoDetection for installing and maintaining their Ion-Q+ equipment at DF1 and DF2. We are grateful to Mahala Ebery for organizing and facilitating the installation and maintenance of the monitoring sites at DF1 and DF2, and to Sophie Golding Chan for the assistance during the maintenance trips. We also thank Paul Reich and John White for their assistance in providing us with spatial data. During the preparation of this work, the authors used OpenAI ChatGPT to check grammar and refine language in parts of the manuscript. After using this tool, the authors reviewed and revised the content and take full responsibility for the content of the publication. Open access publishing facilitated by Monash University, as part of the

Wiley - Monash University agreement via the Council of Australasian University Librarians.

Funding

This work was supported by the Australian Research Council (LP190100755) as well as industry partner funding and in-kind support from West Gippsland Catchment Management Authority, Southern Rural Water, Victorian Government Department of Energy, Environment, and Climate Action, Agriculture Victoria, and State of Victoria Environmental Protection Authority. The first author acknowledges the financial support of the Philippine Department of Science and Technology (DOST) through the Engineering Research and Development for Technology (ERDT) program.

Conflicts of Interest

The authors declare no conflicts of interest.

Data Availability Statement

The data that support the findings of this study are available from the corresponding author upon reasonable request.

References

Aarons, S. R., C. J. P. Gourley, and J. M. Powell. 2023. "Estimating Excreted Nutrients to Improve Nutrient Management for Grazing System Dairy Farms." *Animals* 13, no. 8: 8. https://doi.org/10.3390/ani13081404.

Abbasi, F., J. Simunek, M. T. van Genuchten, et al. 2003. "Overland Water Flow and Solute Transport: Model Development and Field-Data Analysis." *Journal of Irrigation and Drainage Engineering* 129, no. 2: 71–81. https://doi.org/10.1061/(ASCE)0733-9437(2003)129:2(71).

Adams, R., P. Quinn, N. Barber, and S. Burke. 2020. "Identifying Flow Pathways for Phosphorus Transport Using Observed Event Forensics and the CRAFT (Catchment Runoff Attenuation Flux Tool)." *Water* 12, no. 4: 4. https://doi.org/10.3390/w12041081.

Adimalla, N., Li, P., and Qian, H. 2019. "Evaluation of Groundwater Contamination for Fluoride and Nitrate in Semi-Arid Region of Nirmal Province, South India: A Special Emphasis on Human Health Risk Assessment (HHRA)." *Human and Ecological Risk Assessment: An International Journal* 25, no. 5: 1107–1124. https://doi.org/10.1080/10807039.2018.1460579.

Ali, G. A., A. G. Roy, M.-C. Turmel, and F. Courchesne. 2010. "Source-To-Stream Connectivity Assessment Through End-Member Mixing Analysis." *Journal of Hydrology* 392, no. 3: 119–135. https://doi.org/10.1016/j.jhydrol.2010.07.049.

Appels, W. M., P. W. Bogaart, and S. E. A. T. M. van der Zee. 2011. "Influence of Spatial Variations of Microtopography and Infiltration on Surface Runoff and Field Scale Hydrological Connectivity." *Advances in Water Resources* 34, no. 2: 303–313. https://doi.org/10.1016/j.advwatres.2010.12.003.

Appels, W. M., P. W. Bogaart, and S. E. A. T. M. van der Zee. 2016. "Surface Runoff in Flat Terrain: How Field Topography and Runoff Generating Processes Control Hydrological Connectivity." *Journal of Hydrology* 534: 493–504. https://doi.org/10.1016/j.jhydrol.2016.01.021.

Barlow, K., J. Fenton, D. Nash, and R. Grayson. 2006. "Modelling Phosphorus Transport in a Surface Irrigation Drain." *Advances in Water Resources* 29, no. 9: 1383–1398. https://doi.org/10.1016/j.advwatres.2005.10.015.

Barlow, K., D. Nash, M. Hannah, and F. Robertson. 2007. "The Effect of Fertiliser and Grazing on Nitrogen Export in Surface Runoff From Rain-Fed and Irrigated Pastures in South-Eastern Australia." *Nutrient Cycling in Agroecosystems* 77, no. 1: 69–82. https://doi.org/10.1007/s10705-006-9046-6.

Bernal, S., A. Butturini, and F. Sabater. 2006. "Inferring Nitrate Sources Through End Member Mixing Analysis in an Intermittent Mediterranean Stream." *Biogeochemistry* 81, no. 3: 269–289. https://doi.org/10.1007/s10533-006-9041-7.

Bujak-Ozga, I., J. von Freyberg, A. Rinaldo, and I. van Meerveld. 2025. "Comparison of the Dynamics of the Flowing Drainage Network and Water Chemistry for Four Headwater Catchments." *Ecohydrology* 18, no. 2: e2734. https://doi.org/10.1002/eco.2734.

Carpenter, S. R., N. F. Caraco, D. L. Correll, R. W. Howarth, A. N. Sharpley, and V. H. Smith. 1998. "Nonpoint Pollution of Surface Waters With Phosphorus and Nitrogen." *Ecological Applications* 8, no. 3: 559–568. https://doi.org/10.1890/1051-0761(1998)008%5B0559:NPOSWW%5D2.0.CO;2.

Casey, R. E., M. D. Taylor, and S. J. Klaine. 2001. "Mechanisms of Nutrient Attenuation in a Subsurface Flow Riparian Wetland." *Journal of Environmental Quality* 30, no. 5: 1732–1737. https://doi.org/10.2134/jeq2001.3051732x.

Catsamas, S., B. Shi, M. Wang, J. Xiao, P. Kolotelo, and D. McCarthy. 2023. "A Low-Cost Radar-Based IoT Sensor for Noncontact Measurements of Water Surface Velocity and Depth." *Sensors* 23, no. 14: 14. https://doi.org/10.3390/s23146314.

Chalar, G., P. Garcia-Pesenti, M. Silva-Pablo, C. Perdomo, V. Olivero, and R. Arocena. 2017. "Weighting the Impacts to Stream Water Quality in Small Basins Devoted to Forage Crops, Dairy and Beef Cow Production." *Limnologica* 65: 76–84. https://doi.org/10.1016/j.limno.2017.06.002.

Christophersen, N., and R. P. Hooper. 1992. "Multivariate Analysis of Stream Water Chemical Data: The Use of Principal Components Analysis for the End-Member Mixing Problem." *Water Resources Research* 28, no. 1: 99–107. https://doi.org/10.1029/91WR02518.

Christophersen, N., C. Neal, R. P. Hooper, R. D. Vogt, and S. Andersen. 1990. "Modelling Streamwater Chemistry as a Mixture of Soilwater End-Members—A Step Towards Second-Generation Acidification Models." *Journal of Hydrology, Transfer of Elements Through the Hydrological Cycle* 116, no. 1: 307–320. https://doi.org/10.1016/0022-1694(90)90130-P.

Dai, M., Y. Zhao, F. Chai, et al. 2023. "Persistent Eutrophication and Hypoxia in the Coastal Ocean." *Cambridge Prisms: Coastal Futures* 1: e19. https://doi.org/10.1017/cft.2023.7.

Darracq, A., G. Lindgren, and G. Destouni. 2008. "Long-Term Development of Phosphorus and Nitrogen Loads Through the Subsurface and Surface Water Systems of Drainage Basins." *Global Biogeochemical Cycles* 22, no. 3: GB3022. https://doi.org/10.1029/2007GB003022.

Dendup, T., D. Tshering, S. Tobgay, and F. Liu. 2024. "Sources and Pathways of Spring Flow and Climate Change Effects in the Dungju Ri & Yude Ri Catchments, Bhutan Himalaya." *Heliyon* 10, no. 16: e36211. https://doi.org/10.1016/j.heliyon.2024.e36211.

Destouni, G., K. Persson, C. Prieto, and J. Jarsjö. 2010. "General Quantification of Catchment-Scale Nutrient and Pollutant Transport Through the Subsurface to Surface and Coastal Waters." *Environmental Science & Technology* 44, no. 6: 2048–2055. https://doi.org/10.1021/es902338y.

Eco Detection. 2025. "Eco Detection." https://ecodetection.com/what-is-it/.

Edith Allaire, S., E. van Bochove, J.-T. Denault, et al. 2011. "Preferential Pathways of Phosphorus Movement From Agricultural Land to Water Bodies in the Canadian Great Lakes Basin: A Predictive Tool." *Canadian Journal of Soil Science* 91, no. 3: 361–374. https://doi.org/10.4141/cjss09121.

Fenton, O., P. Rice, J. G. Murnane, P. Tuohy, and K. Daly. 2022. "Dairy Farm Roadway Surface Materials as a P-Source Within the Nutrient Transfer Continuum Framework." *Frontiers in Environmental Science* 10: 878166. https://doi.org/10.3389/fenvs.2022.878166.

Finger, L., T. Thayalakumaran, S. Longley, and G. Kaine. 2018. "Assessing Lifestyle, Productive and Environmental Consequences of Tailwater Reuse in the Shepparton Irrigation Region, Australia." *Agricultural Water Management* 205: 50–62. https://doi.org/10.1016/j.agwat.2018.04.028.

Fleming, N. K., J. W. Cox, D. J. Chittleborough, and C. B. Dyson. 2001. "An Analysis of Chemical Loads and Forms in Overland Flow From Dairy Pasture in South Australia." *Hydrological Processes* 15, no. 3: 393–405. https://doi.org/10.1002/hyp.154.

Ford, W. I., A. Husic, A. Fogle, and J. Taraba. 2019. "Long-Term Assessment of Nutrient Flow Pathway Dynamics and in-Stream Fate in a Temperate Karst Agroecosystem Watershed." *Hydrological Processes* 33, no. 11: 1610–1628. https://doi.org/10.1002/hyp.13427.

Franzluebbers, A. J., J. A. Stuedemann, and D. H. Franklin. 2012. "Water Infiltration and Surface-Soil Structural Properties as Influenced by Animal Traffic in the Southern Piedmont USA." *Renewable Agriculture and Food Systems* 27, no. 4: 256–265. https://doi.org/10.1017/S1742170511000378.

Galloway, C., B. Conradie, H. Prozesky, and K. Esler. 2018. "Opportunities to Improve Sustainability on Commercial Pasture-Based Dairy Farms by Assessing Environmental Impact." *Agricultural Systems* 166: 1–9. https://doi.org/10.1016/j.agsy.2018.07.008.

Ghimire, C. P., W. M. Appels, L. Grundy, W. Ritchie, S. Bradley, and V. Snow. 2021. "Towards Predicting the Initiation of Overland Flow From Relatively Flat Agricultural Fields Using Surface Water Coverage." *Journal of Hydrology* 596: 126125. https://doi.org/10.1016/j.jhydrol.2021.126125.

Gray, C. W., C. P. Ghimire, R. W. McDowell, and R. W. Muirhead. 2022. "The Impact of Cattle Grazing and Treading on Soil Properties and the Transport of Phosphorus, Sediment and *E. coli* in Surface Runoff From Grazed Pasture." *New Zealand Journal of Agricultural Research* 65, no. 6: 445–462. https://doi.org/10.1080/00288233.2021.1910319.

Hively, W. D., R. B. Bryant, and T. J. Fahey. 2005. "Phosphorus Concentrations in Overland Flow From Diverse Locations on a New York Dairy Farm." *Journal of Environmental Quality* 34, no. 4: 1224–1233. https://doi.org/10.2134/jeq2004.0116.

Hoekstra, N. J., R. P. O. Schulte, P. J. Forrestal, et al. 2020. "Scenarios to limit environmental nitrogen losses from dairy expansion." *Science of the Total Environment* 707: 134606. https://doi.org/10.1016/j.scitotenv.2019.134606.

Hofmeister, K., R. Lerch, C. Baffaut, J. Yang, and F. Liu. 2022. "Characterizing Groundwater Chemistry and Recharge in the Critical Zone of an Agricultural Claypan Watershed." *Water Resources Research* 58, no. 10: e2021WR031797. https://doi.org/10.1029/2021WR031797.

Holz, G. K. 2010. "Sources and Processes of Contaminant Loss From an Intensively Grazed Catchment Inferred From Patterns in Discharge and Concentration of Thirteen Analytes Using High Intensity Sampling." *Journal of Hydrology* 383, no. 3: 194–208. https://doi.org/10.1016/j.jhydrol.2009.12.036.

Hooper, R. P. 2003. "Diagnostic Tools for Mixing Models of Stream Water Chemistry." *Water Resources Research* 39, no. 3: 1055. https://doi.org/10.1029/2002WR001528.

Hooper, R. P., N. Christophersen, and N. E. Peters. 1990. "Modelling Streamwater Chemistry as a Mixture of Soilwater End-Members—An Application to the Panola Mountain Catchment, Georgia, U.S.A." *Journal of Hydrology, Transfer of Elements Through the Hydrological Cycle* 116, no. 1: 321–343. https://doi.org/10.1016/0022-1694(90)90131-G.

Lindgren, G. A., G. Destouni, and A. Darracq. 2007. "Inland Subsurface Water System Role for Coastal Nitrogen Load Dynamics and Abatement Responses." *Environmental Science & Technology* 41, no. 7: 2159–2164. https://doi.org/10.1021/es062535j.

Liu, F., R. C. Bales, M. H. Conklin, and M. E. Conrad. 2008. "Streamflow Generation From Snowmelt in Semi-Arid, Seasonally Snow-Covered, Forested Catchments, Valles Caldera, New Mexico." *Water Resources Research* 44, no. 12: W12443. https://doi.org/10.1029/2007WR006728.

Liu, F., R. N. Lerch, J. Yang, and G. Peters. 2020. "Determining Hydrologic Pathways of Streamflow Using Geochemical Tracers in a Claypan Watershed." *Hydrological Processes* 34, no. 11: 2494–2509. https://doi.org/10.1002/hyp.13743.

Liu, F., R. Parmenter, P. D. Brooks, M. H. Conklin, and R. C. Bales. 2008. "Seasonal and Interannual Variation of Streamflow Pathways and Biogeochemical Implications in Semi-Arid, Forested Catchments in Valles Caldera, New Mexico." *Ecohydrology* 1, no. 3: 239–252. https://doi.org/10.1002/eco.22.

Liu, F., M. W. Williams, and N. Caine. 2004. "Source Waters and Flow Paths in an Alpine Catchment, Colorado Front Range, United States." *Water Resources Research* 40, no. 9: W09401. https://doi.org/10.1029/2004WR003076.

Luz Rodríguez-Blanco, M., Mercedes Taboada-Castro, M., Teresa Taboada-Castro, M., and Oropeza-Mota, J.L. 2009. "Nutrient Dynamics During Storm Events in an Agroforestry Catchment." *Communications in Soil Science and Plant Analysis* 40, no. 1–6: 889–900. https://doi.org/10.1080/00103620802697921.

Ma, B. L., T. Y. Wu, N. Tremblay, et al. 2010. "On-Farm Assessment of the Amount and Timing of Nitrogen Fertilizer on Ammonia Volatilization." *Agronomy Journal* 102, no. 1: 134–144. https://doi.org/10.2134/agronj2009.0021.

Mackie, C., J. Levison, A. Binns, and I. O'Halloran. 2021. "Groundwater-Surface Water Interactions and Agricultural Nutrient Transport in a Great Lakes Clay Plain System." *Journal of Great Lakes Research* 47, no. 1: 145–159. https://doi.org/10.1016/j.jglr.2020.11.008.

McDowell, R. W., J. J. Drewry, R. W. Muirhead, and R. J. Paton. 2003. "Cattle Treading and Phosphorus and Sediment Loss in Overland Flow From Grazed Cropland." *Australian Journal of Soil Research* 41, no. 8: 1521–1532. https://doi.org/10.1071/SR03042.

McDowell, R. W., K. A. Macintosh, and C. Depree. 2023. "Linking the Uptake of Best Management Practices on Dairy Farms to Catchment Water Quality Improvement Over a 20-Year Period." *Science of the Total Environment* 895: 164963. https://doi.org/10.1016/j.scitotenv.2023.164963.

McGechan, M. B., D. R. Lewis, and P. S. Hooda. 2005. "Modelling Through-Soil Transport of Phosphorus to Surface Waters From Livestock Agriculture at the Field and Catchment Scale." *Science of the Total Environment, Linking Landscape Sources of Phosphorus and Sediment to Ecological Impacts in Surface Waters* 344, no. 1: 185–199. https://doi.org/10.1016/j.scitotenv.2005.02.015.

McGrath, G. S., C. Hinz, and M. Sivapalan. 2009. "A Preferential Flow Leaching Index." *Water Resources Research* 45, no. 11: W11405. https://doi.org/10.1029/2008WR007265.

McHale, M. R., J. J. McDonnell, M. J. Mitchell, and C. P. Cirmo. 2002. "A Field-Based Study of Soil Water and Groundwater Nitrate Release in an Adirondack Forested Watershed." *Water Resources Research* 38, no. 4: 2-1–2–16. https://doi.org/10.1029/2000WR000102.

Monaghan, R. M., P. L. Carey, R. J. Wilcock, et al. 2009. "Linkages Between Land Management Activities and Stream Water Quality in a Border Dyke-Irrigated Pastoral Catchment." *Agriculture, Ecosystems & Environment* 129, no. 1: 201–211. https://doi.org/10.1016/j.agee.2008.08.017.

Mulholland, P. J., and W. R. Hill. 1997. "Seasonal Patterns in Streamwater Nutrient and Dissolved Organic Carbon Concentrations: Separating Catchment Flow Path and In-Stream Effects." *Water Resources Research* 33, no. 6: 1297–1306. https://doi.org/10.1029/97WR00490.

Mundy, G. N., K. J. Nexhip, N. R. Austin, and M. D. Collins. 2003. "The Influence of Cutting and Grazing on Phosphorus and Nitrogen in Irrigation Runoff From Perennial Pasture." *Soil Research* 41, no. 4: 675–685. https://doi.org/10.1071/SR02087.

Murphy, D. J., P. Dillon, M. O' Donovan, L. Shalloo, and E. Ruelle. 2024. "Nitrate Leaching on Irish Grassland Dairy Farms: A Review." *European Journal of Agronomy* 153: 127042. https://doi.org/10.1016/j.eja.2023.127042.

Nash, D., L. Clemow, M. Hannah, K. Barlow, and P. Gangaiya. 2005. "Modelling Phosphorus Exports From Rain-Fed and Irrigated Pastures in Southern Australia." *Soil Research* 43, no. 6: 745–755. https://doi.org/10.1071/SR04119.

Nash, D., B. Webb, M. Hannah, et al. 2007. "Changes in Nitrogen and Phosphorus Concentrations in Soil, Soil Water and Surface Run-Off Following Grading of Irrigation Bays Used for Intensive Grazing." *Soil Use and Management* 23, no. 4: 374–383. https://doi.org/10.1111/j.1475-2743.2007.00100.x.

Nazari, S., W. I. Ford, and K. W. King. 2021. "Quantifying Hydrologic Pathway and Source Connectivity Dynamics in Tile Drainage: Implications for Phosphorus Concentrations." *Vadose Zone Journal* 20, no. 5: e20154. https://doi.org/10.1002/vzj2.20154.

Norton, J., and Y. Ouyang. 2019. "Controls and Adaptive Management of Nitrification in Agricultural Soils." *Frontiers in Microbiology* 10: 1931. https://doi.org/10.3389/fmicb.2019.01931.

Oenema, J., and O. Oenema. 2021. "Intensification of Grassland-Based Dairy Production and Its Impacts on Land, Nitrogen, and Phosphorus Use Efficiencies." *Frontiers of Agricultural Science and Engineering* 8, no. 1: 1. https://doi.org/10.15302/J-FASE-2020376.

Oldham, C. E., D. E. Farrow, and S. Peiffer. 2013. "A Generalized Damköhler Number for Classifying Material Processing in Hydrological Systems." *Hydrology and Earth System Sciences* 17, no. 3: 1133–1148. https://doi.org/10.5194/hess-17-1133-2013.

Pedregosa, F., G. Varoquaux, A. Gramfort, et al. 2018. "Scikit-learn: Machine Learning in Python (arXiv:1201.0490)." arXiv. https://doi.org/10.48550/arXiv.1201.0490.

Peterson, E. E., F. Sheldon, R. Darnell, S. E. Bunn, and B. D. Harch. 2011. "A Comparison of Spatially Explicit Landscape Representation Methods and Their Relationship to Stream Condition." *Freshwater Biology* 56, no. 3: 590–610. https://doi.org/10.1111/j.1365-2427.2010.02507.x.

Porter, V. M., J. B. Shanley, S. D. Sebestyen, and F. Liu. 2022. "Controls on Decadal, Annual, and Seasonal Concentration-Discharge Relationships in the Sleepers River Research Watershed, Vermont, Northeastern United States." *Hydrological Processes* 36, no. 3: e14559. https://doi.org/10.1002/hyp.14559.

Rasiah, V., J. D. Armour, and P. N. Nelson. 2013. "Nitrate in Shallow Fluctuating Groundwater Under Sugarcane: Quantifying the Lateral Export Quantities to Surface Waters." *Agriculture, Ecosystems & Environment, Catchments to Reef Continuum: Minimising Impacts of Agriculture on the Great Barrier Reef* 180: 103–110. https://doi.org/10.1016/j.agee.2012.07.002.

Sądej, W., and K. Przekwas. 2008. "Fluctuations of Nitrogen Levels in Soil Profile Under Conditions of a Long-Term Fertilization Experiment." *Plant, Soil and Environment* 54, no. 5: 197–203. https://doi.org/10.17221/394-PSE.

Smith, V. H., G. D. Tilman, and J. C. Nekola. 1999. "Eutrophication: Impacts of Excess Nutrient Inputs on Freshwater, Marine, and Terrestrial Ecosystems." *Environmental Pollution* 100, no. 1: 179–196. https://doi.org/10.1016/S0269-7491(99)00091-3.

Song, J.-H., Y. Her, and T. Guo. 2022. "Quantifying the Contribution of Direct Runoff and Baseflow to Nitrogen Loading in the Western Lake Erie Basins." *Scientific Reports* 12, no. 1: 9216. https://doi.org/10.1038/s41598-022-12740-1.

State of Victoria Department of Transformation and Planning. 2025. "Vicmap 1-m DEM [Digital Elevation Model]."

Tauro, F., G. Olivieri, A. Petroselli, M. Porfiri, and S. Grimaldi. 2016. "Flow Monitoring With a Camera: A Case Study on a Flood Event in the Tiber River." *Environmental Monitoring and Assessment* 188, no. 2: 118. https://doi.org/10.1007/s10661-015-5082-5.

Tesoriero, A. J., T. B. Spruill, H. E. Mew Jr., K. M. Farrell, and S. L. Harden. 2005. "Nitrogen Transport and Transformations in a Coastal Plain Watershed: Influence of Geomorphology on Flow Paths and Residence Times." *Water Resources Research* 41, no. 2: W02008. https://doi.org/10.1029/2003WR002953.

Tian, C., X. Zhou, Z. Ding, et al. 2021. "Controlled-Release N Fertilizer to Mitigate Ammonia Volatilization From Double-Cropping Rice." *Nutrient Cycling in Agroecosystems* 119, no. 1: 123–137. https://doi.org/10.1007/s10705-020-10108-3.

van der Salm, C., A. van den Toorn, W. J. Chardon, and G. F. Koopmans. 2012. "Water and Nutrient Transport on a Heavy Clay Soil in a Fluvial Plain in The Netherlands." *Journal of Environmental Quality* 41, no. 1: 229–241. https://doi.org/10.2134/jeq2011.0292.

Van Gaelen, N., D. Verheyen, B. Ronchi, et al. 2014. "Identifying the Transport Pathways of Dissolved Organic Carbon in Contrasting Catchments." *Vadose Zone Journal* 13, no. 7: vzj2013.11.0199–vzj2013.11.0114. https://doi.org/10.2136/vzj2013.11.0199.

van Meter, K. J., and N. B. Basu. 2017. "Time Lags in Watershed-Scale Nutrient Transport: An Exploration of Dominant Controls." *Environmental Research Letters* 12, no. 8: 084017. https://doi.org/10.1088/1748-9326/aa7bf4.

van Verseveld, W. J., J. J. McDonnell, and K. Lajtha. 2008. "A Mechanistic Assessment of Nutrient Flushing at the Catchment Scale." *Journal of Hydrology* 358, no. 3: 268–287. https://doi.org/10.1016/j.jhydrol.2008.06.009.

Vogeler, I., S. Thomas, and T. van der Weerden. 2019. "Effect of Irrigation Management on Pasture Yield and Nitrogen Losses." *Agricultural Water Management* 216: 60–69. https://doi.org/10.1016/j.agwat.2019.01.022.

Wan, L., A. D. Kendall, S. L. Martin, Q. F. Hamlin, and D. W. Hyndman. 2023. "Important Role of Overland Flows and Tile Field Pathways in Nutrient Transport." *Environmental Science & Technology* 57, no. 44: 17061–17075. https://doi.org/10.1021/acs.est.3c03741.

Watanabe, K., Y. Minami, M. Iguchi, and Y. Fujita. 2024. *Robust and Accurate River Flow Measurement by Space-Time Image Velocimetry (STIV) With Improved Deep Learning Technique*. 1st ed, 8. CRC Press.

West Gippsland Catchment Management Authority. 2018. "Lake Wellington Land and Water Management Plan." https://wgcma.vic.gov.au/wp-content/uploads/2023/03/WGCMA-LWMP-Jan2019-FULL-final-web.pdf.

Wilcock, R. J., D. Nash, J. Schmidt, S. T. Larned, M. R. Rivers, and P. Feehan. 2011. "Inputs of Nutrients and Fecal Bacteria to Freshwaters From Irrigated Agriculture: Case Studies in Australia and New Zealand." *Environmental Management* 48, no. 1: 198–211. https://doi.org/10.1007/s00267-011-9644-1.

Wild-Allen, K., and J. Andrewartha. 2016. "Connectivity Between Estuaries Influences Nutrient Transport, Cycling and Water Quality." *Marine Chemistry, 13th International Estuarine Biogeochemistry Symposium (IEBS)—Estuaries Under Anthropogenic Pressure* 185: 12–26. https://doi.org/10.1016/j.marchem.2016.05.011.

Williams, M. R., S. J. Livingston, C. J. Penn, et al. 2018. "Controls of Event-Based Nutrient Transport Within Nested Headwater Agricultural

Watersheds of the Western Lake Erie Basin." *Journal of Hydrology* 559: 749–761. https://doi.org/10.1016/j.jhydrol.2018.02.079.

Wu, Y., X. Shi, C. Li, S. Zhao, F. Pen, and T. R. Green. 2017. "Simulation of Hydrology and Nutrient Transport in the Hetao Irrigation District, Inner Mongolia, China." *Water (Switzerland)* 9, no. 3: 169. https://doi.org/10.3390/w9030169.

Xiao, Y., D. Xiao, Q. Hao, et al. 2021. "Accessible Phreatic Groundwater Resources in the Central Shijiazhuang of North China Plain: Perspective From the Hydrogeochemical Constraints." *Frontiers in Environmental Science* 9: 747097. https://doi.org/10.3389/fenvs.2021.747097.

Zhang, Y., and X. Zhang. 2009. "Experimental Analysis of the Effective Depth of Interaction of Rainfall-Surface Runoff-Soil Nitrogen." In *2009 3rd International Conference on Bioinformatics and Biomedical Engineering*, 1–5. Institute of Electrical and Electronics Engineers (IEEE). https://doi.org/10.1109/ICBBE.2009.5162813.

Supporting Information

Additional supporting information can be found online in the Supporting Information section. **Figure S1:** Matrix plots of ion (Cl^-, F^-, PO_4^{3-}, SO_4^{2-}, K^+, Na^+) concentrations measured by the Eco Detection equipment from the farm drain discharge at DF1. All solute concentrations are reported in mg/L. **Figure S2:** Matrix plots of major ion (Cl^-, F^-, PO_4^{3-}, SO_4^{2-}, K^+, Na^+) concentrations measured from the farm drain discharge at DF2. All solute concentrations are reported in mg/L. **Figure S3:** Calculation of total microtopographic depression storage for (a–e) DF1 and (f–j) DF2. **Figure S4:** Time series of (a) discharge, rainfall, and irrigation inputs; (b) end member contributions, and; (c–j) nutrient/solute concentrations (reported in mg/L) in farm drain water at DF1. **Figure S5:** Time series of (a) discharge, rainfall, and irrigation inputs; (b) end member contributions, and; (c–j) nutrient/solute concentrations (reported in mg/L) in farm drain water at DF2.